Fall 2011

Contrast enhancement of digital mammography based on multi-scale analysis

Muhammad Imran Khan Abir

Department:

CONTRAST ENHANCEMENT OF DIGITAL MAMMOGRAPGY BASED ON MULTI-SCALE ANALYSIS

by

MUHAMMAD IMRAN KHAN ABIR

A THESIS

Presented to the Faculty of the Graduate School of the

MISSOURI UNIVERSITY OF SCIENCE AND TECHNOLOGY

In Partial Fulfillment of the Requirements for the Degree

MASTER OF SCIENCE IN NUCLEAR ENGINEERING

2011

Approved by

Hyoung Koo Lee, Advisor

Arvind Kumar

Shoaib Usman

Randy H. Moss

PUBLICATION THESIS OPTION

This thesis consists of the journal article that will be submitted for publication to EURASIP Journal on Advances in Signal Processing. Pages 1-43 of this thesis will be regenerated for writing the journal article on EURASIP.

ABSTRACT

A contrast enhancement algorithm is developed for digital mammograms aiming to assist radiologists in discerning early breast cancer easily. The algorithm is based on a Laplacian pyramid framework image processing technique. The mammogram is decomposed into three frequency sub-bands, low, mid, and high frequency sub-band images. The lower sub-band image contains very fine details and higher level contains coarser features. In this method contrast enhancement is achieved from high and mid sub-bands by decomposing the image based on multi-scale Laplacian pyramid and enhance contrast by image processing. Several mapping functions are applied on sub-band images based on experimental analysis. After modifying sub-band images using mapping functions, the final image is derived from reconstruction of the Laplacian images from lower resolution level to upper resolution level. To demonstrate the effectiveness of the algorithm, two mammogram images are analyzed. To validate the algorithm, quantitative measurements are performed. Several existing contrast enhancement techniques are compared with the developed algorithm. Experimental results and quantitative evaluation prove that the proposed algorithm offers improved contrast of digital mammograms.

ACKNOWLEDGMENTS

I am especially grateful to Dr. Hyoung Koo Lee for giving me the opportunity to pursue research providing with scientific guidance, constant support and sharing his knowledge relating to image processing.

I would also like to thank Dr. Randy H. Moss for sharing his vast knowledge on image processing and Matlab. I also thank Dr. Shoaib Usman and Dr. Randy H. Moss for being a member of my thesis defense and Dr. Arvind Kumar, the department chair for his support of my research.

I would also like to show gratitude to NRC faculty development fund for supporting me during my M.S. studies.

I would not forget my roommate and friend, Siddhartha Biswas, who gave me unforgettable help during my tough situation in my M.S. study.

Finally, I would like to acknowledge my family members: my father, Muhammad Abdur Rashid Khan, my mother Afroza Akther, have supported me in every moment, and my wife ‘Tamanna’ for encouraging my work.

TABLE OF CONTENTS

LIST OF ILLUSTRATIONS

LIST OF TABLES

ABBREVIATIONS

Acronyms	Description
CAD	Computer Aided Diagnosis
CCD	Charged Coupled Device
CLAHE	Contrast Limited Adaptive Histogram Equalization
CNR	Contrast-to-Noise Ratio
DSM	Distribution Separation Measure
FFDM	Full Field Digital Mammography
HE	Histogram Equalization
MUSICA	Multi-scale Image Contrast Amplification
MIAS	Mammographic Image Analysis Society
QC	Quality Control
ROI	Region Of Interest
SFM	Screen Film Mammography
SNR	Signal-to-Noise Ratio
TBC_s	Target-to-Background Contrast enhancement measure based on Standard deviation
TBC_e	Target-to-Background Contrast enhancement measure based on Entropy

1. INTRODUCTION

Breast cancer is a heterogeneous progressive asymptomatic disease of women all over the world. It develops from within the branching ductal system of the breast. About 1 in 8 women in the United States (12%) develops invasive breast cancer of her lifetime. In 2010, an estimated 207,090 new cases of invasive breast cancer were expected to be diagnosed in women in the U.S., along with 54,010 new cases of non-invasive breast cancer [2]. About 39,840 women in the U.S. were expected to die in 2010 from breast cancer. Breast cancer can be developed in different areas of the breast- the ducts, the lobules or even the tissue in between. From 2000, digital mammography has become the superior over film mammography due to better contrast, resolution and dynamic range.

In x- ray imaging like digital mammography, enhancement of low contrast features is necessary since most of the important features are barely seen by the human eye. Contrast enhancement helps the radiologist to visualize features and diagnose disease more accurately. Contrast enhancement can be done globally and locally. Global contrast enhancement changes image contrast regardless of image contents. In digital mammography local contrast enhancement methods are more suitable because of the size and non-uniformity of the digital mammogram. Like all other x-ray images, mammographic images have histograms of similar shape. Two sets of components that dominate in the histogram of the image, one is the background that has gray values near zero and the other is the object. For contrast enhancement, either global or local, the background should be removed to make the background gray level distribution narrower. Contrast enhancement is necessary for making microcalcification stand out from the breast tissue in a dense breast.

This thesis is organized in the following way. Section 2 describes the theory and background of the thesis. This includes a synopsis of screen film mammography and digital mammography and recent advances of contrast enhancement. Section 3 describes the method of the proposed image processing algorithm. Detail explanation of the process and mathematical derivation of applying the method is presented. Section 4 contains the result and analysis of the algorithm. Experimental analysis and quantitative evaluation is demonstrated in this section. Section 5 presents the comparison of the proposed technique

with traditional well-known image processing techniques. Section 6 presents the concluding remarks of this thesis. The code of this algorithm is in appendix section. For generating the code MATLAB is used.

2. BACKGROUND

2.1. USE OF X-RAY IN MEDICAL IMAGING

X-rays were discovered by William Roentgen (1895) while experimenting with a cathode radiation. In the health and medical areas, x-rays have been used for both diagnosis and treatment of patients' conditions for over a century. X-rays are used in a wide variety of examinations in diagnostic medical imaging. Some applications of x-ray in medical images are illustrated in Table 2.1:

Table 2.1. Applications of x-ray in medical imaging

General Radiography	Single projection images of chests, skull, spines, breasts, etc
Fluoroscopy	Single projection images to display continuous x-ray images like x-ray movie
Angiography	Series of single projection images to view body's blood vessels
Computed Tomography	Multiple projection imaging system to view anatomical cross sections
Bone Mineral Densitometry	Multiple projection imaging to measure the density of minerals per cubic centimeter of bones

2.2. SCREEN FILM MAMMOGRAPHY

A set of screening mammogram actually consists of two x-ray images, one taken from the side (called as "mediolateral oblique view") and the other from above (called as "craniocaudal view") for each breast. . The mammographic process involves exposure of the breast to x-rays of mammographic energies (kVp) followed by the transmission and scattering of x-rays through breast tissue (Figure 2.1).

Screening mammography has been shown to reduce breast cancer mortality by approximately 18%–30% in the past decade [18].

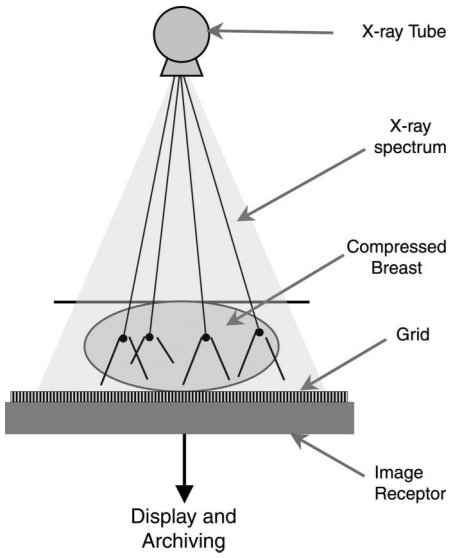

Figure 2.1. Typical process of screen film mammography [18]

Due to high-quality images obtained with screen-film mammography (SFM) systems, the mortality rate for breast cancer has been reduced. SFM systems are considered the standard of reference in diagnosing breast cancer. But approximately 10%–20% of breast cancers detected at breast self-examination or physical examination are not visible to SFM. However, only 5%–40% of the lesions detected with SFM and recommended for biopsy are found to be malignant [14]. This indicates a high level of false-positives, resulting in unnecessary biopsies and related psychological stress to patients.

The attenuated x-ray photons pass through the grid and interact with the image receptor. The photons are finally absorbed as a latent image on the film. After processing, the film is then displayed for diagnosis. The entire process is captured, displayed, and archived with a single medium, which is the film. The SFM has some inherent advantages, mentioned in [12]:

1. High spatial resolution (up to 20 line pairs per millimeter), which can demonstrate fine spiculation and microcalcification.
2. High contrast, which allows visualization of subtle differences among soft-tissue densities [14].
3. Use of high-luminance view boxes, which improves visualization of dense tissues.

4. Ease of display, rearrangement, and masking of film during diagnosis, which allows simultaneous display of images made during screening examinations and supplementary views of previous images on multiple panel illuminators.
5. Use of multiple image receptor sizes enables imaging breasts of different sizes.
6. Film acts as an efficient medium for long-term storage with low cost.

Although SFM has some advantages, there are a number of inherent limitations with SFM. The major disadvantage of SFM is the limited dynamic range as shown in Figure 2.2. There are trade-offs between dynamic range and contrast resolution, noise due to film granularity, and compromise between resolution and efficiency.

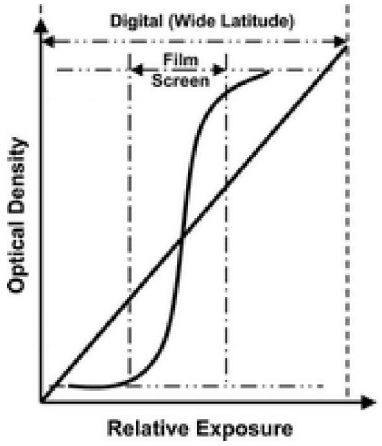

Figure 2.2. Comparison of dynamic range between SFM and digital mammography [18]

The film acts as the only medium for acquisition, display, and storage of images. Image quality can be affected by suboptimal condition of any step and limit the full capability of the mammography process. The limitation of SFM is explained in Figure 2.3, which is composed of wide range of tissues.

From Figure 2.3, it can be demonstrated that, while the system is optimized for the dense part of the breast, all other tissues fall on the upper plateau of the film response curve, making them impossible to visualize.

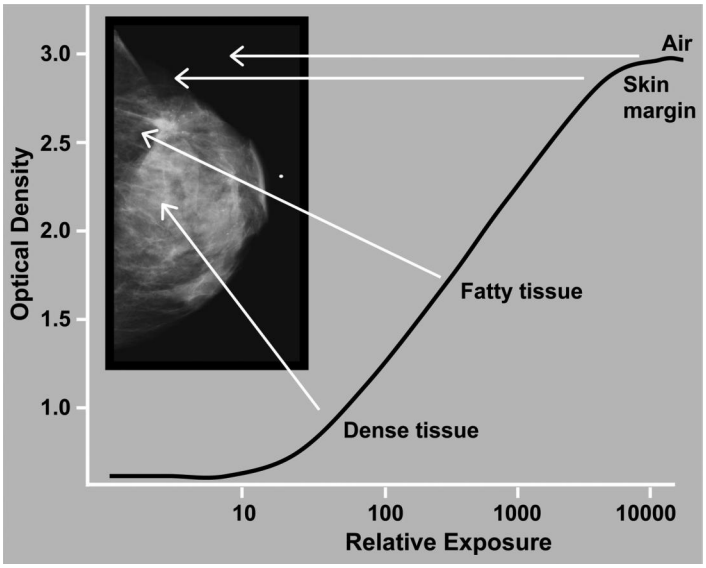

Figure 2.3. Different regions of the breast image are represented according to the characteristic response of a typical mammographic film [18]

In addition, technical factors such as film processing, developing, and image artifacts can limit the use of SFM. Digital mammography has the potential to overcome the limitations of SFM and improve early breast cancer detection and lesion characterization.

2.3. DIGITAL MAMMOGRAPHY

Mammograms can be delivered in a digital format in two different ways: Conventional screen-film mammograms (SFM) can be converted to a digital image, referred to as a digitized film screen mammogram. Furthermore, mammograms can be generated as a digital image directly, referred to as a direct full-field digital mammogram (FFDM). Both systems are distinguishable as the images are generated in two different ways.

For the development of FFDM systems, various approaches have been taken as described in [18], [22], [30]. The system can be classified as direct or indirect system. Indirect capture uses a two-step process whereby a scintillator such as cesium iodide (CsI) absorbs the x-rays and generates a light scintillation which is similar to SFM. The scintillation is then detected by an array of photodiodes or charge-coupled devices (CCDs). With the direct capture process, the x-ray photons are directly captured by a

photoconductor such as amorphous selenium (a-Se) and converts absorbed x-rays to a digital signal [1]. The possibilities of resolution degradation due to light spread at indirect capture are eliminated in these systems. Moreover, the spatial resolution with direct capture is limited to the pixel size and not to the thickness of the photoconductor.

The physics of x-ray image acquisition in mammography can be demonstrated through a simple model of a breast containing a structure of interest. The structure of interest might be a tumor, a microcalcification, or some normal aspect of the breast anatomy. For a monoenergetic x-ray beam, the mean number of x-rays transmitted along path '*A*' through normal breast tissue and arriving at a hypothetical plane beyond the breast, referred to as the image plane, is [23]:

$$n_A = n_0 e^{-\mu X} \tag{1}$$

where n_0 is the mean number of x-rays incident on the breast, X is the thickness, and μ is the x-ray attenuation coefficient of the tissue.

Assuming that the divergence of x-rays from a point source has been ignored and no scattered radiation reaches the image plane. The number of x-rays that are transmitted along path '*B*' (Figure 2.4.) is passing through the structure of interest in the breast having x-ray linear attenuation coefficient, μ' is:

$$n_B = n_0 e^{-\mu(X-a)-\mu' a} \tag{2}$$

Where a is the thickness of the structure in the direction of travel of the x-rays.

The signal difference produced by the presence of the structure is:

$$SD = n_A - n_B \tag{3}$$

The resultant radiation contrast is:

$$C_{rad} = \frac{n_A - n_B}{n_A + n_B} \tag{4}$$

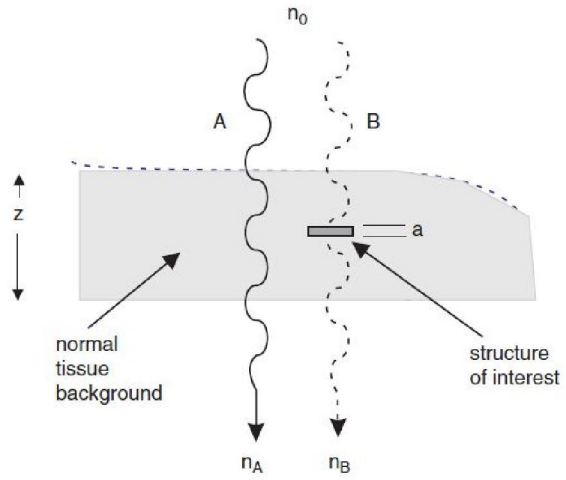

Figure 2.4. Schematic diagram of the breast illustrating the basic imaging problem of detecting differences in x-ray transmission between path *A* passing through normal tissue and path *B* passing through a region containing a structure of interest such as a lesion in a breast of varying thickness [24].

Substituting eq. (1) and eq. (2) into eq. (4), we can get:

$$C_{rad} = \frac{1-e^{-(\mu-\mu')a}}{1+e^{-(\mu-\mu')a}} \tag{5}$$

This expression shows that the radiation contrast is determined by two factors, the difference in the attenuation coefficient between the background breast tissue and the structure and the thickness of the structure.

If a mammogram is converted into a digital format, the image can be manipulated in a variety of ways to highlight lesion conspicuity. The radiologist can alter the orientation, magnification, brightness and contrast of the images as desired. Digital images can be viewed in several ways, such as on a high-luminance computer monitor or printed as a film. From the patient's point of view, mammography with a digital system is essentially the same as with the screen-film system. Unlike SFM, digital images can be stored and transferred electronically, which facilitates their quick and easy retrieval as well as allowing remote evaluation by distant specialists. The outcomes proposed for measuring the efficacy of digital mammography are the potential to detect breast cancer at an earlier

stage, reduce the number of false positive mammograms, decreased radiation dose to the breast, increased accuracy of images, facilitation of long distance consultations with mammography specialists, and ease of mammography storage.

2.4. ADVANTAGES OF DIGITAL MAMMOGRAPHY

The advances in digital detectors offer improved detection due to the improved efficiency of absorption of incident x-ray photons. Some of the inherent advantages of digital detectors are the linear response over a wide range of x-ray intensities and low system noise. The processes of image acquisition, displaying, and archiving is decoupled which provides an opportunity to independently optimize each process. Wide dynamic range (1,000:1) compared with that of SFM (40:1), dynamic image manipulation, and the ability to postprocess, which allows improvement in lesion visibility are some of the advantages of digital mammography. The overall mammography process can be improved by soft-copy reading accompanied by computer-aided diagnosis (CAD) and three-dimensional imaging [18].

A well-optimized digital mammography system can provide the following benefits [22]:

1. More efficient acquisition of the x-ray data for the mammogram because
    (a) The detector can be made thick enough to absorb a large fraction of the x-rays transmitted by the breast
    (b) Granularity noise should be eliminated.
    (c) Radiation dose should be reduced.
2. The image data is captured in numerical form.
3. Display brightness and contrast can be controlled.
4. For adapting the image to match visual performance of the eye and overcome limitations of the display device image processing can be performed.
5. Able to remove other structural noises by flat-field correction.

2.5. CONTRAST ENHANCEMENT OF DIGITAL MAMMOGRAPHY

The purpose of contrast enhancement is to enhance image feature against its background to visualize the image properties in an open eye. X-ray beam is used for digital

mammography and the x-ray density controls the relevant detail information of the mammogram. The patient should not get more doses. Less exposure reduces patient dose as well as image contrast. Suitable image processing for contrast enhancement can reconcile the limitation. Pertinent information remains in the high frequency region of mammogram but the large density variation mostly crop up in low frequencies. Contrast enhancement enhances the high frequency information of an image while suppressing the unnecessary low frequency information thus visualizes the subtle information of the digital mammogram. The digital format of digital mammography allows image processing to be applied to digital images without additional exposure to the patient. Contrast enhancement is one such technique whereby the contrast of different structures in the breast is altered to improve detectability. Image processing also involves edge enhancement or smoothing the image and zooming in on a suspicious region in an image for better viewing. Image enhancement can be divided into types: direct and indirect contrast enhancement.

2.5.1. Direct Contrast Enhancement. Direct contrast enhancement establishes a criterion of contrast measure and enhances the images by improving the contrast directly. Establishment of a suitable image contrast measure is the key step of direct image enhancement. Local contrast is measured by using the mean gray values in two rectangular windows centered on a given pixel.

2.5.1.1. Optimal adaptive neighborhood contrast enhancement. The direct contrast enhancement algorithm is based on measurement of local contrast. The method takes a neighbor consisting of a square of coefficients surrounding the center of a given coefficient. The center pixel is called the center of the neighborhood and a large annulus called the surround. The contrast measure is defined by [8]

$$C = \frac{|p-a|}{|p+a|} \qquad \text{where } 0 \leq C \leq 1 \tag{6}$$

where p is the average density of the center and 'a' is the average density of the surround. The contrast value for each pixel was transformed to a new contrast value by using a suitable contrast enhancement function. The enhanced contrast can be obtained by replacing the old pixel value with enhanced pixel values.

2.5.1.2. Adaptive fuzzy logic contrast enhancement. In fuzzy logic approach both global and local contrast can be enhanced. The method is based on fuzzy entropy principle which transforms the image to a fuzzy domain, and computes the fuzzy entropy and measures the local contrast. The histogram provides the global information of the contrast. Finally, the enhanced image can be obtained by defuzzification to transform the enhanced mammogram from fuzzy domain to spatial domain.

2.5.1.3. Contrast enhancement in the wavelet domain. A local contrast measure for direct contrast enhancement can also be described in wavelet domain. The contrast values are manipulated in the wavelet domain by using high frequency and low frequency information. The contrast value is defined by the ratio of the bandpass filtered image at that frequency to which the image lowpass-filtered to an octave below the same frequency. A contrast manipulation factor is used to enhance the measured contrast value. The image is reconstructed by using inverse wavelet transform and the enhanced mammogram can be seen. The inherent advantage of the proposed algorithm is that, this technology can be applied to JPEG2000 compressed image in the decompression stage to reduce the time required for enhancement. Also this technology matches the human visual system which results a better visual quality.

2.5.2. Indirect Contrast Enhancement. Indirect contrast enhancement cannot manipulate the image contrast directly; rather it modifies the histogram or high frequency image and thus increases contrast. Several methods are being adopted for indirect contrast enhancement of digital images.

2.5.2.1. Contrast stretching. Contrast stretching improves an image contrast by stretching the range of intensity values uniformly. It expands the full intensity range of the recording medium [11] as shown in Figure 2.5.

If *f (x, y)* is the original image and *a* and *b* are the lower and upper limits of the desired stretching respectively and *c* and *d* are the maximum and minimum gray value of the original image respectively then the contrast stretching can be defined as:

$$f'(x,y) = a + \frac{b-a}{d-c} * [f(x,y) - c] \quad (7)$$

This is the type of global contrast enhancement. For digital image processing local contrast enhancement is more suitable, so the method is not widely used in digital mammography.

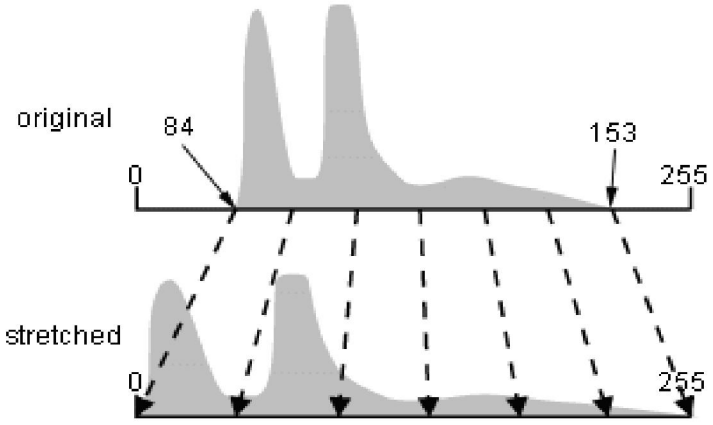

Figure 2.5. Linear contrast stretching

2.5.2.2. Histogram equalization. In histogram equalization, the high contrast appearance can be achieved by distributing the image pixels to the entire intensity levels that is increasing the dynamic range of the histogram of the image. The overall contrast improvement can be achieved by flattens and stretched the dynamic range of the histogram of the image. Histogram equalization can be applied on the digital mammograms but since this method enhances the contrast globally so there are losses of details outside the denser parts of the image.

Some modification of histogram equalization has been performed on recent days. For example bi-histogram equalization [32], recursive mean separate histogram equalization [4], minimum mean brightness error histogram equalization [5], partially overlapped sub-block histogram equalization [15], etc. Those methods are well established for optical images but they are not suitable for digital mammography.

2.5.2.3. Adaptive histogram equalization. In this method, based on local neighborhood, a different grayscale transform is computed at each location in the image, and the pixel value at that location is mapped accordingly. The local window is selected as

a square tile centered at the pixel to be processed. The regions occupy different gray scale ranges and those would be enhanced locally by using histogram equalization. In order to eliminate the artificial boundaries created by the process, interpolation is necessary across the block regions. Contrast can be increased by changing the slope of the transform that converts pixel values from the original to the processed image. With adaptive histogram equalization, noise will be increased to an unacceptable level in image regions that have little signal variation, that is, homogeneously dense tissue areas or background. This is the inherent problem of this technique [1].

2.5.2.4. Contrast limited adaptive histogram equalization. To reduce contrast amplification in dense breast tissue or background, contrast limited adaptive histogram equalization (CLAHE) has been proposed. The slope of the transform computed by histogram equalization is proportional to the height of the histogram. The slope can be limited by clipping and renormalizing the histogram before computing the transform. Maximum contrast enhancement can be adjusted by introducing an additional parameter. But CLAHE does not give the performance of the algorithm in fatty areas of the breast [24].

2.5.2.5. Unsharp masking. Unsharp masking is a well recognized image sharpening method in digital image processing. Recently this method was attributed on digital mammography to enhance mammographic feature. In this method, a low pass filtered version of the original image is subtracted from the latter and the resultant image is multiplied by a weighing factor. This multiplied image is to be added to the original image to get the enhanced version of the image. The sharpness of the border of mass lesion will be enhanced in this method but it has some inherent limitations. The details and noise are obvious in this method and in the high contrast areas some undesirable overshoot artifacts can be generated [31].

2.5.3. Multiscale Contrast Enhancement. For tuning contrast enhancement to certain frequency bands it is possible to use multi-scale image processing. Enhance of contrast can be done at different scales. It is possible to enhance micro-calcifications and masses in a range of scales, while suppressing other structures. Two well-known multi-scale processing are: wavelet transform and Laplacian pyramid.

2.5.3.1. Multiscale wavelet based enhancement. A common multi-scale processing technique is wavelet based enhancement. Laine et al first proposed the multi-scale wavelet based enhancement of digital mammography in 1994 [16]. A wavelet transform is a decomposition of an image onto a family of functions called wavelet family. This decomposition divides the frequency spectrum of an image into a low pass sub-band image and a set of band pass sub-band images which contain the wavelet coefficients. Research has been performed on both discrete and continuous wavelets [13].The wavelet coefficients can be modified locally or globally by suitable enhancement functions. In both cases, edges and gain parameters are identified adaptively by a measure of energy within each level of scale space [16]. Mammograms are reconstructed from modified wavelet coefficients modified at one or more levels. Adaptive wavelet based enhancement had been proposed in [16] where an adaptive denoising and contrast enhancement was proposed together. For contrast enhancement, non-linear modification on wavelet coefficient based on non-linear gain operator was presented. Wavelet processing can reveal features that are barely seen in unprocessed traditional mammograms [17]. However, the clinical benefit of displaying such features has not been demonstrated.

2.5.3.2. Laplacian based enhancement. The Laplacian Pyramid was first introduced for image compression [3]. Multi-scale image contrast amplification (MUSICA^{TM}) [29] is a well-known technique for contrast enhancement by using Laplacian Pyramid. The method used a power law with a linear lower and upper cutoff. The lower cutoff value was introduced to avoid too strong amplification of noise and is the upper limit for the nonlinear contrast enhancement. MUSICA^{TM} used the same remapping parameters in all sub-bands, but in [28] Stahl et al. introduced a remapping function with a variation of the gain in all sub-bands. These special features include noise robustness and a density-dependent enhancement. In [9] it was shown that for the enhancement of radiographs, decomposition by wavelet transform leads to undesirable artifacts in the enhanced images. The Laplacian Pyramid decomposition is a more suitable decomposition method for multiscale enhancement, since it is free from such artifacts and results in a very balanced image impression.

3. METHOD

The proposed contrast enhancement algorithm is based on a multi - scale Laplacian pyramid. Pyramid representations are the decomposition of the image combining with subsampling and smoothing operation. Laplacian Pyramid signifies the image into a set of the different sub-band images. The purpose of using Laplacian decomposition is that most digital mammogram contains subtle information; it is difficult to enhance features from one frequency band.

3.1. MULTISCALE IMAGE DECOMPOSITION

The concept of scale in an image is mostly used in image and video processing. Scale corresponds to the amount of details and resolution corresponds to the size of details that can be perceived by an observer. An image consists of two types of scale: *coarse* scale and *fine* scale. Original shapes and general features lie on the coarse scales of the image and detail structures and indistinguishable features lie on fine scales. The purpose of multiscale decomposition is to separate coarse and fine scales of an image and extracting important features from the fine scales. The advantage of using multiscale decomposition is the ability to modify coarse scales and fine scales separately. The separation into coarse and fine scales has a wide application in image processing that include image segmentation [25], image registration [19], pattern recognition, medical image reconstruction [7], etc.

The key factor of overall performance and quality of decomposition depends on the selection of smoothing operator. Two main requirements are needed for selecting a good smoothing filter [20]. First, the filter spectrum has to be smooth and band-limited in the frequency domain, and the other is the spatial localization constraint on the filter characteristics. This means that pixels in the smoothed image should be computed from the weighted average of nearby pixels. The first requirement introduces ringing artifacts which can be prevented by the second requirement. Gaussian like filter is the best possible smoothing filter that fulfills the requirements.

3.1.1. Gaussian Pyramid. The Gaussian pyramid is the representation of an image at different scales and at different resolutions. The Gaussian pyramid can be generated by convolving the image with a 2-D Gaussian lowpass kernel and subsamples it by a factor of

2. The pyramid decomposes an image into a hierarchy of low pass filtered images such that successive levels correspond to lower frequencies.

If I_0 denotes the original image then $G_0 = I_0$ is the first level of the Gaussian pyramid. The next level, G_1, is computed by convolving G_0 with a Gaussian filter kernel and down sampling it by a factor of 2. The Gaussian pyramid for l-th level is computed by:

$$G_l = REDUCE\ (G_{l-1}); \qquad l \geq 1 \tag{8}$$

where the *REDUCE* is an operator which represents the convolution with the filter kernel and down-sampling by a factor of 2. Therefore, if the size of the original image I_0 is $2^N \times 2^M$, then G_l has size $2^{N-l} \times 2^{M-l}$.

The 2-D Gaussian filter can be expressed as:

$$w(m,n) = \frac{1}{2\pi\sigma^2} e^{-\frac{m^2+n^2}{2\sigma^2}} \tag{9}$$

The parameter σ determines the size of the filter. The degree of smoothing increases with the increase of the kernel or scale size but the bandlimit of the image decreases. the image can be reduced proportionally to this bandlimit without losing any information. The filter kernel is typically chosen to be a 5 × 5 pattern of weights. If the kernel is denoted by w, then the *REDUCE* operation can be written as:

$$G_l(x,y) = \sum_{m=-2}^{2} \sum_{n=-2}^{2} w\,(m,n) \times G_{l-1}(2x+m, 2y+n) \tag{10}$$

The kernel will satisfy the following constraints [21]:

1. The kernel w would be separable: $w\,(x, y) = \hat{w}(x)\,\hat{w}(y)$ which denotes that the filter can be implemented as the cascade of 1-D filters operating along columns and rows.

2. The one dimensional filter $\hat{w}$ is normalized.

$$\sum_{x=-2}^{2} \hat{w}(x) = 1 \tag{11}$$

3. The one dimensional filter $\hat{w}$ is symmetric: $\hat{w}(i) = \hat{w}(-i)$ for $i = 0, 1, 2$.
4. All pixels at a given level must contribute equally to pixels at the next level. This is shown in Figure 3.1

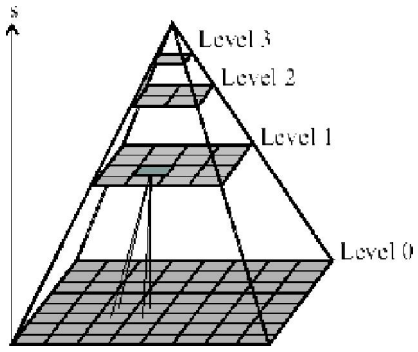

Figure 3.1. Pyramidal structure of the image

The Gaussian Pyramid represents a smoothed version of the original image at each level. Figure 3.2 illustrates the first five levels of the Gaussian pyramid of a mammogram image selected from the Mammographic Image Analysis Society (MIAS) database.

3.1.2. Laplacian Pyramid. The convolution of the original image with a Gaussian kernel is a lowpass filtering operation with the bandlimit reduced correspondingly by one octave with each level [10]. A Laplacian image is the difference between the two levels of the Gaussian pyramid and the Laplacian pyramid is a sequence of the differences L_0, $L_1, \ldots, L_n$. The adjacent levels G_l and G_{l+1} in the Gaussian pyramid are of different size, G_{l+1} is expanded to achieve the same size of G_l. This can be obtained by an operator *EXPAND*, which is the reverse of the operator *REDUCE*.

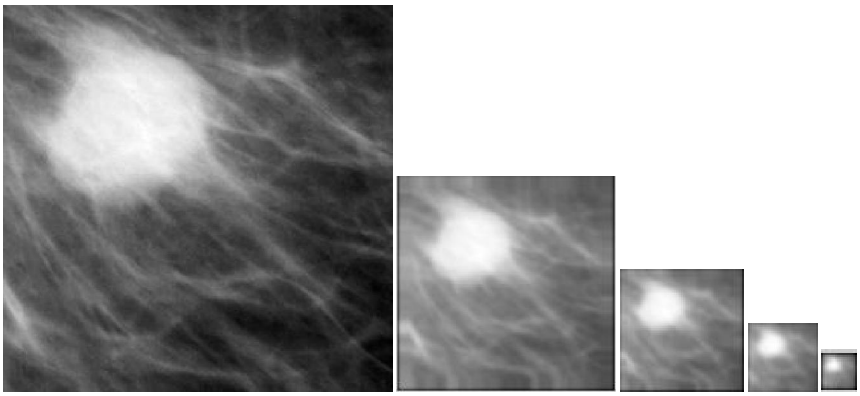

Figure 3.2. The first 5th levels of the Gaussian pyramid of a mammogram cropped in 256×256 size

$$G_l = EXPAND(G_{l+1}) \tag{12}$$

The effect of the *EXPAND* operator is to up-sample the $2^{N-l} \times 2^{M-l}$ image matrix into a $2^{N-l+1} \times 2^{M-l+1}$ array by inserting zeros in between each pixel and convolve it by the Gaussian kernel. If the *EXPAND* operation is applied to image G_l of the Gaussian pyramid, then the resultant image would be an image of size G_{l-1} which has the same size as the image G_{l-1} in the previous level of the Gaussian pyramid. The *EXPAND* operation can be mathematically written as:

$$G_l(x,y) = 4 \sum_{m=-2}^{2} \sum_{n=-2}^{2} w\,(m,n) \times G_{l+1}\left(\frac{x-m}{2}, \frac{y-n}{2}\right) \tag{13}$$

The Laplacian pyramid is obtained by the following formula:

$$L_l = G_l - EXPAND(G_{l+1}) \tag{14}$$

A single level Laplacian image is shown in Figure 3.3

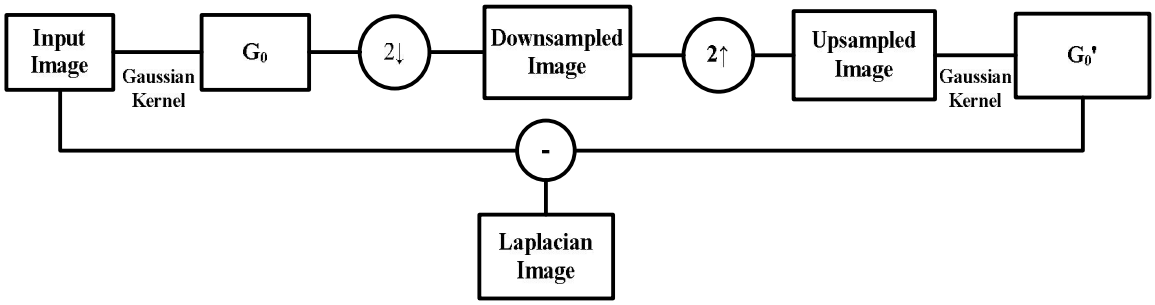

Figure 3.3. Generation of one level Laplacian image

The difference between Gaussian Pyramid and Laplacian Pyramid is that the Gaussian Pyramid smoothes brighter values over larger areas and produces a set of lowpass filtered copies of the original image and the Laplacian Pyramid differentiates smoothed brightness values and produces a set of bandpass filtered copies of the original image.
Figure 3.4 illustrates the first five levels of the Laplacian pyramid of a mammogram image selected from MIAS database.

3.2. MATHEMATICAL DERIVATION

The Laplacian derivative operator is given by:

$$\nabla^2 g(x,y) = \frac{\partial^2 g}{\partial x^2} + \frac{\partial^2 g}{\partial y^2}$$

The 1-D Gaussian kernels can be expressed as:

$$g(x;\sigma) = \frac{1}{\sqrt{2\pi}\sigma} e^{-x^2/2\sigma^2}$$

Differentiating with respect to *x*

$$\frac{dg(x;\sigma)}{dx} = \frac{-x}{\sigma^2} g(x;\sigma)$$

Differentiating with respect to *x* again:

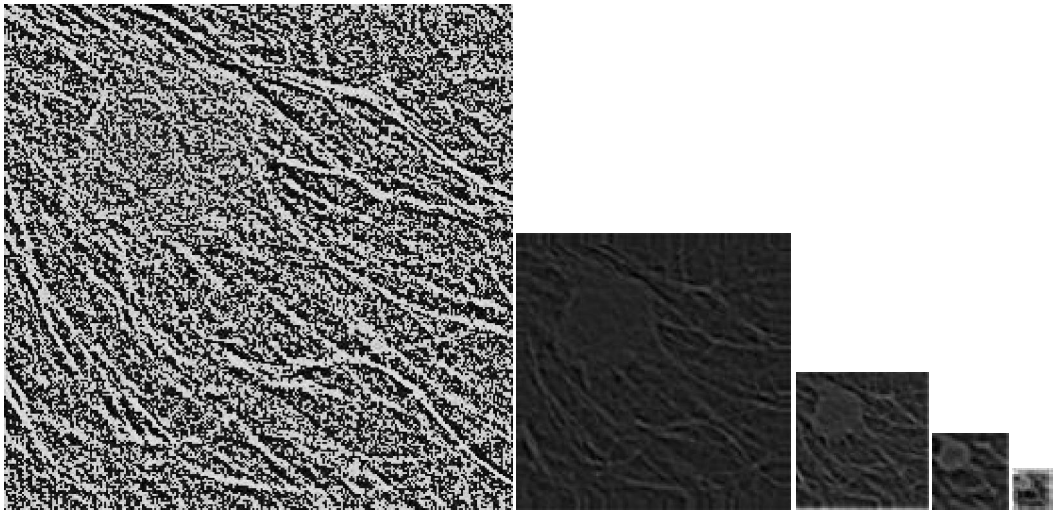

Figure 3.4. The first 5th levels of Laplacian pyramid of a mammogram cropped in 256 × 256 size

$$\frac{d^2 g(x;\sigma)}{dx^2} = \left(\frac{x^2}{\sigma^2} - 1\right)\frac{1}{\sigma^2} g(x;\sigma)$$

Differentiating with respect to σ:

$$\frac{dg(x;\sigma)}{d\sigma} = \left(\frac{x^2}{\sigma^2} - 1\right)\frac{1}{\sigma} g(x;\sigma)$$

Therefore:

$$\begin{aligned}\frac{d^2 g(x;\sigma)}{dx^2} &= c_0(\sigma)\frac{dg(x;\sigma)}{d\sigma} \\ &\approx c_1(\sigma)(g(x;\sigma) - g(x;\sigma + \Delta\sigma))\end{aligned}$$

So, if the low-pass filter used to create the Laplacian Pyramid is Gaussian, then the Laplacian pyramid levels approximate the second derivative of the image at scale σ.

3.3. CONTRAST ENHANCEMENT

3.3.1. Development of Mapping Function. The contrast enhancement was achieved by modifying the Laplacian pyramid coefficients. The Laplacian pyramid images

are a series of different images which contains subtle features of the mammogram. The lowest level of the pyramid contains the high frequency components of the image and the highest level contains low frequency components. Modification at the high frequency coefficients is necessary and the lower frequency coefficient should be attenuated. But, the high frequency coefficients contain fine details as well as noise, so enhancement of high frequency coefficients will enhance fine structures and noise too. The non-linear mapping function has been developed to enhance the high frequency coefficients without amplification of noise. The mapping function that has been developed is:

$$x' = x + \frac{a*sigm\,(x)M\left(\frac{x}{M}\right)^{\gamma}}{K} \tag{15}$$

$$x' = b * x \tag{16}$$

$$x' = c * (M - (2K - x)^{\gamma}) \times \frac{M}{2(M-K)} \tag{17}$$

where x represents the original pyramid coefficient and x' represents the modified coefficients. M is the maximum value of the coefficients of a particular level, a and b are the amplification factors. γ is an exponent that controls the non-linearity of the coefficients. K is the upper bound of the coefficient values. Since high frequency bands contain noise content, so the global amplification factors *a, b, c* and the non-linear exponent γ should be chosen selected accordingly. Laplacian pyramid coefficients contain positive and negative values. The low coefficient values correspond to subtle details in the image, and should be enhanced. Equation (15) and (16) are used for this purpose based on the degree of enhancement. The higher coefficient values should be reduced in order to prevent the blurring effect and noise enhancement. Equation (17) is used for this purpose. The signum is a sign function that extracts the sign of a real number.

3.3.2. Implementation of Mapping Function. The developed mapping function was applied to each level of the Laplacian pyramid. For each level, the maximum value was found from the Laplacian image. For example, if the first level of Laplacian image is L_0, the maximum value of L_0 was selected from the image. Suitable upper bound K was chosen from L_0 and based on the experimental analysis the mapping functions are applied. The global amplification factors *a, b* and *c* are chosen for L_0 and a non-linear exponent was

selected to enhance the coefficient values. By applying the mapping function and selecting proper values for *K, M, γ, a, b* and *c* at each level of Laplacian pyramid, modified Laplacian pyramid was generated. The mapping functions are applied to each level and are shown in Figure 3.5.

The multiscale analysis provides the access of image feature that lie on intermediate bands. The purpose of multiscale processing is to remove unnecessary and disturbing details of the image and enhance the fine details so that calcifications can be more visible in the human visual system. Various multi-scale methods have been already proposed recently as described in 2.4.3, where the image was split up into a number of sub-bands. But, all sub-bands were processed by using single mapping functions. However, different mapping functions were used to visualize subtle important structures of the mammogram. Smaller positive and most negative coefficients carry important information.

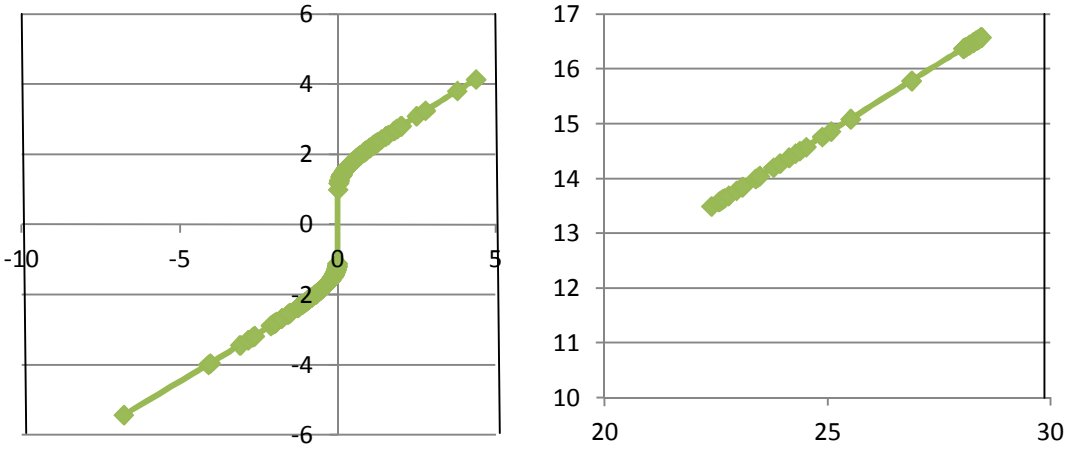

(a) Modified Lower Coefficients at Level 1

(b) Modified Higher Coefficients at Level 1

Figure 3.5. Structure of the mapping function from level 1 to level 5 of the modified Laplacian coefficients

If the positive coefficients are treated similarly as lower coefficient there is more blurring effect on the overall image after reconstruction. So, the higher coefficients should be reduced.

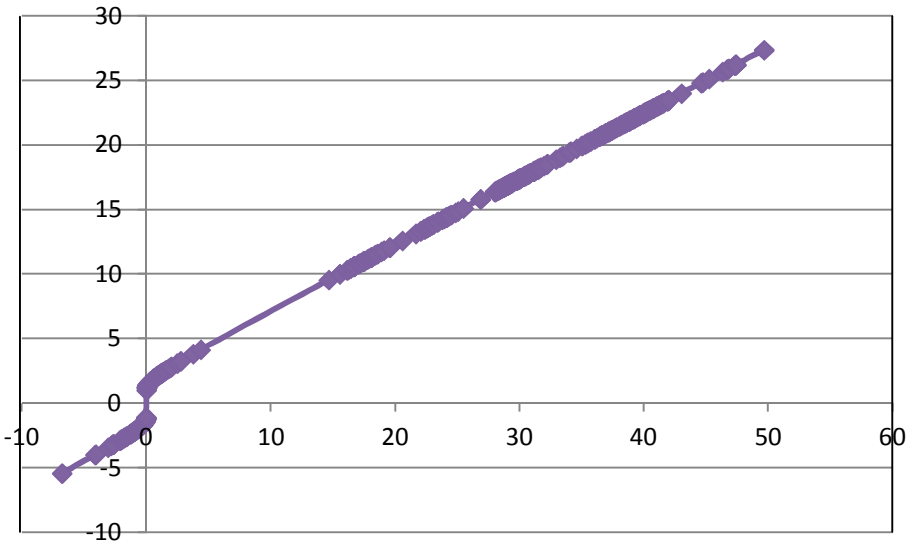

(c)

Modified Coefficients at Level 1

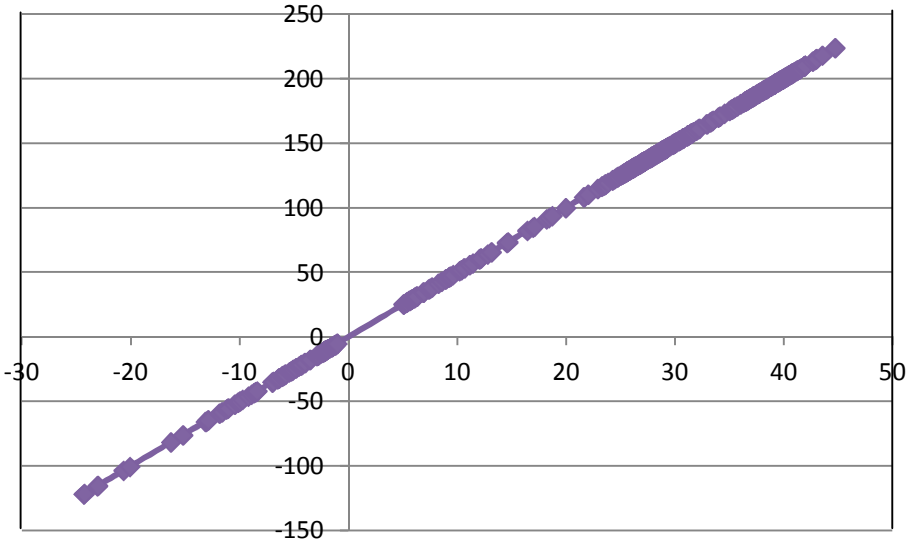

(d)

Modified Coefficients at Level 2

Figure 3.5. Structure of the mapping function from level 1 to level 5 of the modified Laplacian coefficients (cont.)

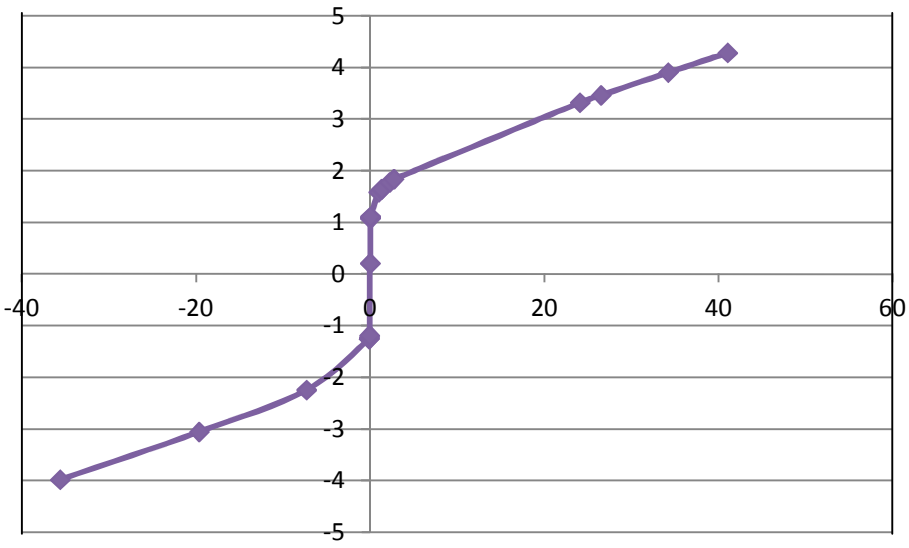

(e)

Modified Coefficients at Level 3

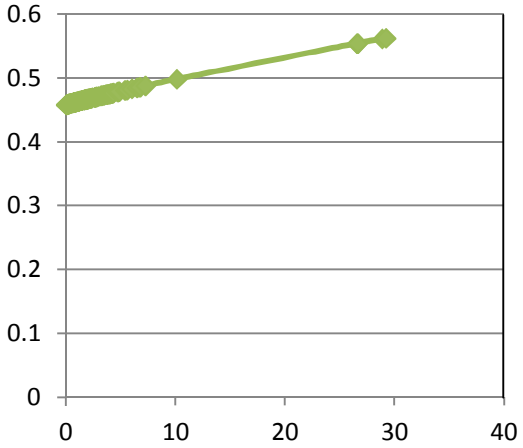

(f)

Modified Higher Coefficients at Level 4

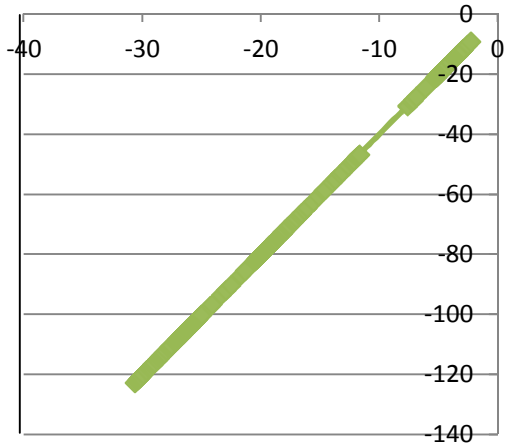

(g)

Modified Lower Coefficients at Level 4

Figure 3.5. Structure of the mapping function from level 1 to level 5 of the modified Laplacian coefficients (cont.)

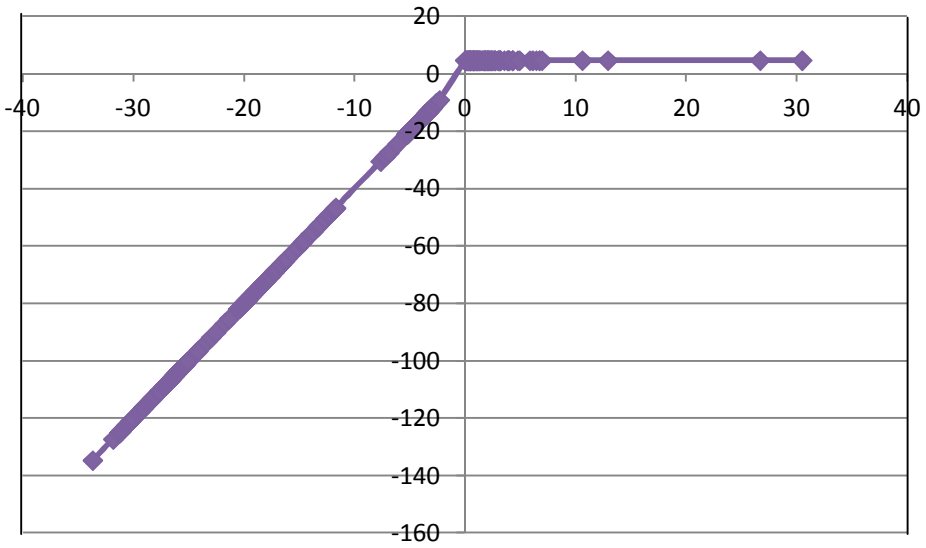

(h)

Modified Coefficients at Level 4

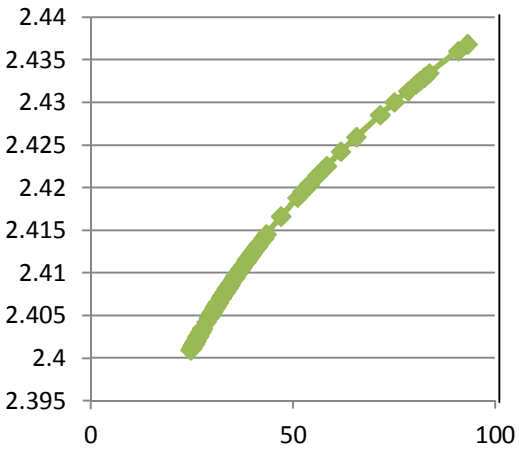

(i)

Modified Higher Coefficients at Level 5

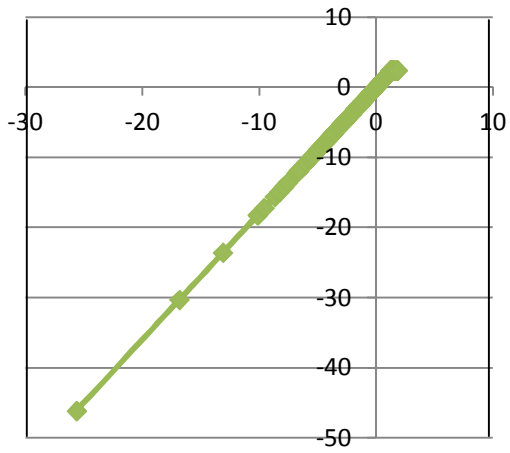

(j)

Modified Lower Coefficients at Level 5

Figure 3.5. Structure of the mapping function from level 1 to level 5 of the modified Laplacian coefficients (cont.)

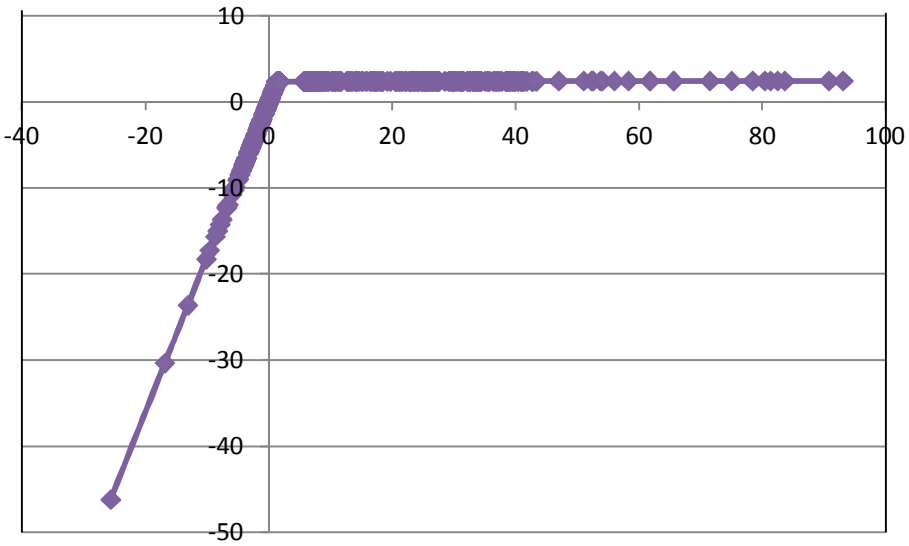

(k)

Modified coefficients at Level 5

Figure 3.5. Structure of the mapping function from level 1 to level 5 of the modified Laplacian coefficients (cont.)

In order to suppress the higher coefficients different mapping function (Eq. 17) was used. Only the first level sub-band L_0 contains subtle features of the image. Therefore, the coefficients of this sub-band should be treated differently. Figures 3.5 (b), (f) and (i) show the attenuation of the higher coefficients. Moreover, the lower positive coefficients and the negative coefficients were enhanced but they were modified differently to enhance the overall contrast of the image as shown in Figure 3.5 (a), (e), (g), (j). From L_1 through L_4 except L_2, the higher positive coefficients were attenuated to reduce the blurring effect and suppressing the noise. Also, the brightness of the overall reconstructed image increases if those positive coefficients are increased. Higher coefficients of L_2 were enhanced same as negative coefficients since it has been observed experimentally that this level contains the most important features of the mammogram and does not enhance brightness much. Lower positive coefficients and all negative coefficients were enhanced based on suitable contrast requirements. The conclusion of this new method would be that this modified technique is more versatile and efficient method than conventional multi-scale methods.

3.4. PYRAMID RECONSTRUCTION

The modified Laplacian pyramid images were reconstructed by using pyramid reconstruction. The residual Gaussian image was upsampled by a factor of 2 and smoothed by the 5×5 Gaussian kernel. The upsampled image was added with the modified Laplacian coefficients of the lowest level of the Laplacian pyramid and a reconstructed image is generated. The image is up-sampled again to its upper resolution level by a factor of 2, smoothed and added to the corresponding level's modified Laplacian image. The operation is repeated up to original image size is obtained. The resultant image is the image that has better contrast than the original image.

The last level of Laplacian Pyramid is shown in Figure 3.6

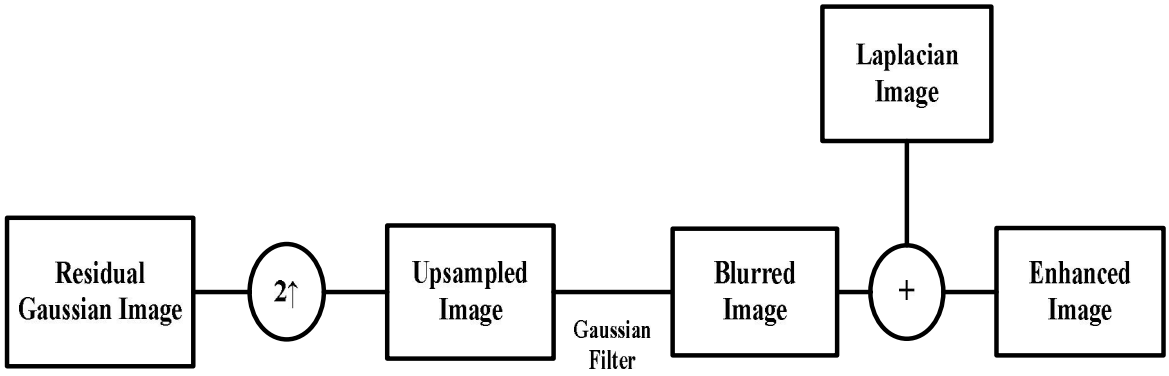

Figure 3.6. Reconstruction of Laplacian image

3.5. FLOW DIAGRAM

The overall structure of the algorithm is shown in Figure 3.7. The diagram shows the five levels of decomposition that is used in this thesis. As described, for each level two mapping functions are used. After applying the mapping function the Laplacian images are reconstructed with the residual Gaussian image. Finally, the output image is formed which has better contrast than the original image. D_0, L_0, L_0', R_0 represents decomposition, Laplacian coefficients, modified Laplacian coefficients and reconstruction respectively. The last level of downsampled image is called Residual image.

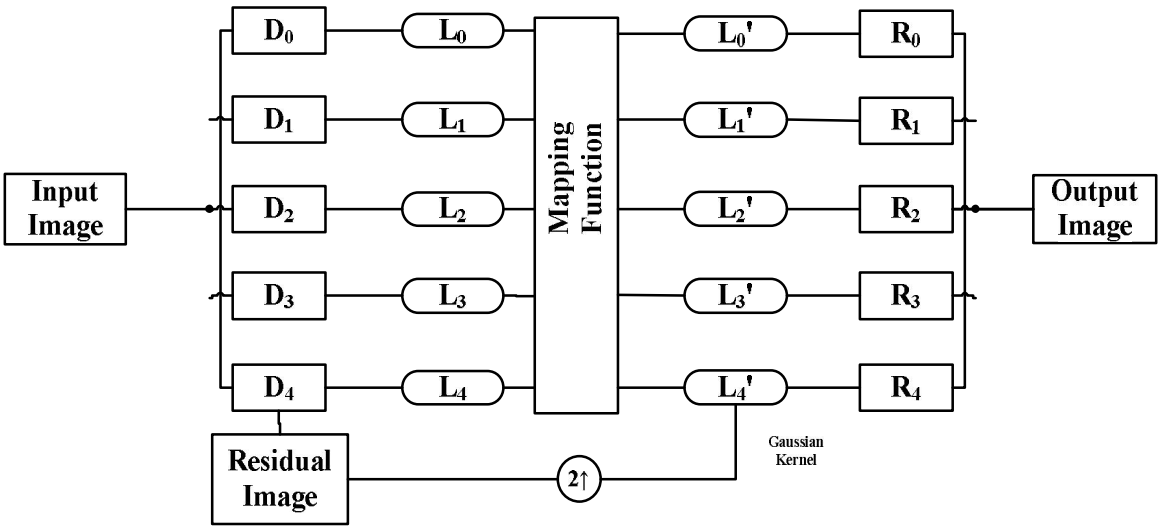

Figure 3.7. Developed algorithm using Laplacian pyramid

3.6. EVALUATION CRITERIA

3.6.1. Signal-to-Noise Ratio (SNR). The signal to noise ratio is the power ratio of the original signal to noise. The original signal is the mean or expected value of the signal whereas the noise is the standard deviation of the signal. The power is expressed as square of the amplitude.

$$SNR = \frac{P_{signal}}{P_{noise}} = \left(\frac{A_{signal}}{A_{noise}}\right)^2 \tag{18}$$

SNR can be measured in decibels.

$$SNR(dB) = 10\ log\frac{P_{signal}}{P_{noise}} = 20\log\left(\frac{A_{signal}}{A_{noise}}\right)^2 \tag{19}$$

3.6.2. Contrast-to-Noise Ratio (CNR). CNR is a measure of ability to visualize physiological structures, lesions, abnormalities of an image. Contrast is a local feature which can be described by the difference between the gray value of the object and the background.

$$C(x,y) = \frac{|f_{object} - f_{background}|}{f_{object} + f_{background}} \quad (20)$$

CNR is expressed as:

$$CNR = \frac{|f_{object} - f_{background}|}{\sigma\,(x,y)} \quad (21)$$

where $\sigma\,(x, y)$ is the standard deviation of noise in an image.

3.6.3. Distribution Separation Measure. For any image, a distribution of target, T and background, B can be plotted as two normal Probability Density Functions (PDF's) with mean and standard deviations. Typically there is an overlap between the two distributions as shown in Figure 3.8 (b). The goal of contrast enhancement technique is to maximize the distance between these two distributions to ensure that the target is visible against the background. A measurement to separate these two PDFs would be an indicator of the performance of the technique. The technique is described in [27].

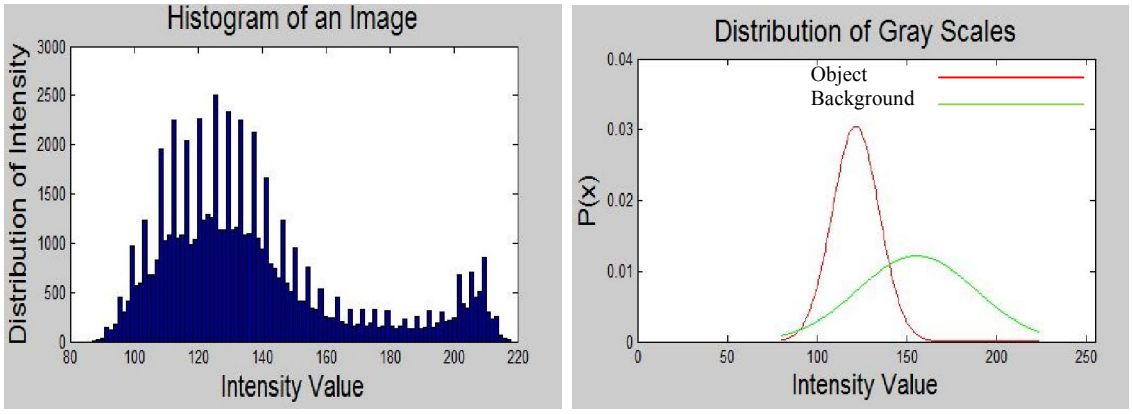

Figure 3.8. (a) shows the histogram of an image, and Figure 3.8 (b) shows the overlapping PDFs of target and background

Mathematically DSM is expressed as:

$$DSM = (|\mu_T^E - \mu_B^E|) + (|\mu_T^O - \mu_B^O|) \quad (22)$$

where μ_T^O and μ_B^O correspond to the mean of target and background before enhancement and μ_T^E and μ_B^Ecorrespond the mean target and background after enhancement. Ideally, DSM value should be greater than zero. Good contrast enhancement reduces the overlap between the spread of target and background distribution, hence maximize the distance between the two distributions.

3.6.4. Target-to-Background Contrast Based on Standard Deviation. Other metrics to evaluate contrast enhancement technique is to maximize the difference between background and target mean gray level. The quantifiable metrics have been developed in [27]:

$$TBC_s = \left\{ \frac{\left(\frac{\mu_T^E}{\mu_B^E}\right) - \left(\frac{\mu_T^O}{\mu_B^O}\right)}{\frac{\sigma_T^E}{\sigma_T^O}} \right\} \quad (23)$$

where μ_T^O, μ_B^O, σ_T^O correspond to the mean and standard deviation of target and background before enhancement and μ_T^E, μ_B^E, σ_T^E correspond the mean and standard deviation of target and background after enhancement. $TBC_s > 0$ represents the enhancement of the image.

3.6.5. Target-to-Background Contrast Based on Entropy. To quantify the homogeneity ratio other metrics used is target-to-background contrast enhancement measurement based on entropy. The concept is similar to TBC_s except that the standard deviation is replaced with the entropy.

$$TBC_e = \left\{ \frac{\left(\frac{\mu_T^E}{\mu_B^E}\right) - \left(\frac{\mu_T^O}{\mu_B^O}\right)}{\frac{\varepsilon_T^E}{\varepsilon_T^O}} \right\} \quad (24)$$

where ε_T^O and ε_T^E are the entropy of the image before and after enhancement respectively. The contrast enhanced image should give TBC_e value greater than 1.

3.6.6. Combined Enhancement Measure. The DSM, TBC_s and TBC_e values are combined together to get a single value D which is another metric of contrast enhancement.

$$D = \sqrt{(1 - DSM)^2 + (1 - TBC_s)^2 + (1 - TBC_e)^2} \tag{25}$$

It is expected that the smallest D value should give best enhancement. The D value compares the enhancement techniques to select the best method for contrast enhancement.

4. RESULTS AND ANALYSIS

4.1. EXPERIMENTAL ANALYSIS

For testing the performance of new algorithm several mammogram images were selected from the Mammographic Image Analysis Society (MIAS) database. The images are digitized to 50 micron pixel edge and reduced to 200 micron pixel edge and padded to make the image 1024×1024 pixels. The algorithm was developed in MATLAB 7.8.0 (R2009a). The computer used was a core i5 CPU with 4.0 GB memory.

Case 1: Fatty tissue with well defined mass.

The first mammogram contains fatty tissue with well-defined mass. The original mammogram and the enhanced mammogram are shown in Figure 4.1 (a) and Figure 4.1 (b) respectively. The histogram of the original image and the enhanced image is shown in Figure 4.2 (a) and Figure 4.2 (b) respectively.

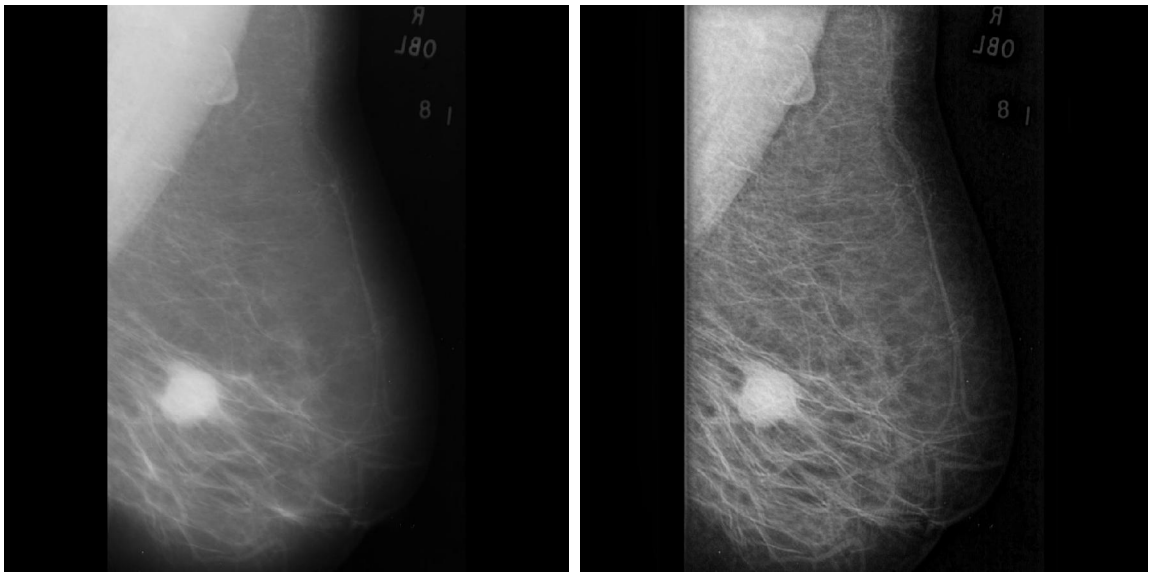

Figure 4.1. (a) shows the original mammogram with fatty tissue and well-defined masses with malignant tumor, and Figure 4.1. (b) shows the processed mammogram

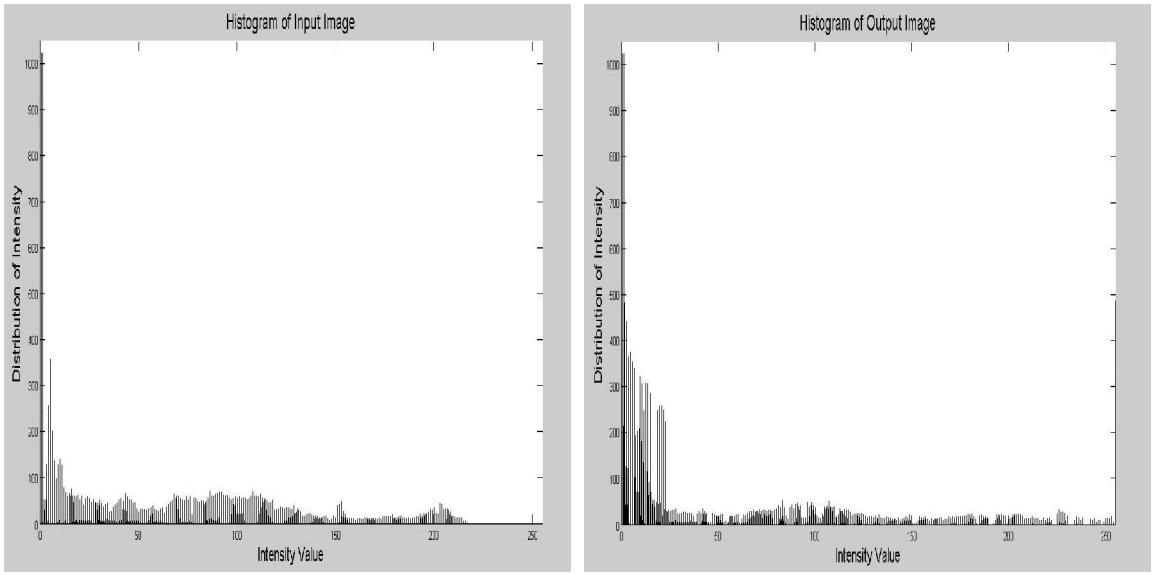

Figure 4.2. (a) shows the histogram of the original image, and Figure 4.2. (b) shows the histogram of the processed image.

It was clearly seen from the image that the lesion and the anatomical structures were obvious in the human visual system. From histogram it can be proved that the intensity values are well distributed which makes the anatomical structure of the mammogram more visible.

In the experiment the level of Laplacian pyramid was five and the 5×5 Gaussian kernel was used at each level to construct the Laplacian pyramid. The purpose of using same Gaussian kernel is to prevent the ringing effect that can give a worse output image. For first level Eq. (15) was used for the low coefficient values and Eq. (16) was used for high coefficient values. For second level Eq. (15) was used but since there was no upper bound, so the maximum coefficient value was used for upper bound. The purpose of avoiding upper bound was analyzed experimentally. It was seen that the second and third level coefficients carry the most important features of the image and the higher positive coefficients should enhance proportionally as the lowest coefficients. At fourth and fifth level, the higher coefficient values mostly contain the edge information of the image and more blurring effect over the image appeared if those coefficients enhance. The reduction of those coefficients has largely increased the contrast of the image as well as sharpens the

edges. Eq. (17) was developed empirically to attenuate the high coefficients. A horizontal scan line profile is created to show the local enhancement of the mammogram which clearly shows the contrast enhancement of the mammogram. Figure 4.3 shows the ROI and the original and processed image and Figure 4.4 shows the line profiles of them.

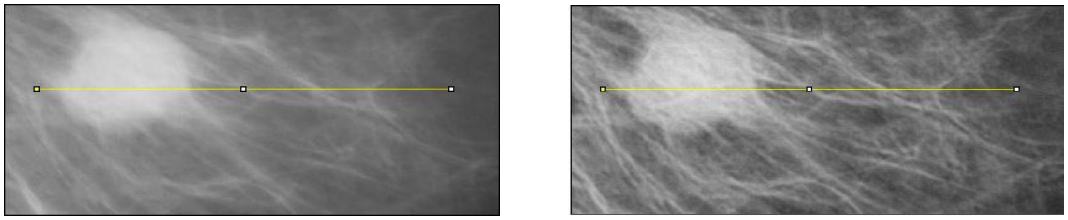

Figure 4.3. (a): ROI of the original image, and Figure 4.3. (b) ROI of the processed image for plotting line profile

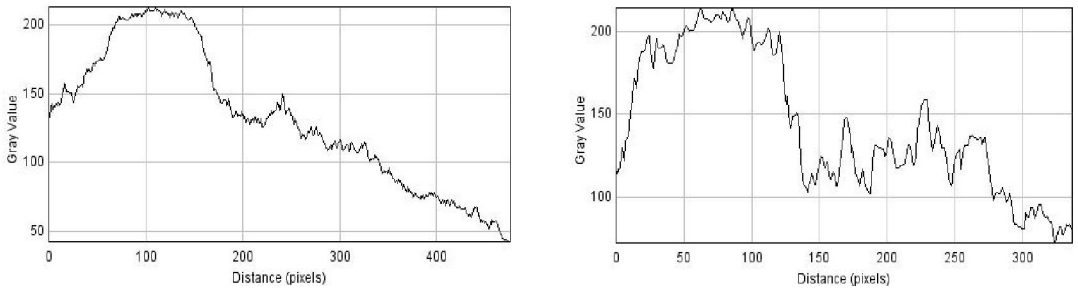

Figure 4.4. (a): shows the line profile of original image, and Figure 4.4. (b) shows the line profile of the processed image

Case 2: Fatty-glandular tissue with calcification

The mammogram contains fatty-glandular tissue with calcification. The original image and the enhanced image are shown in Figure 4.5.

Contrast enhancement is the variation of gray scales of the surrounding gray values. From the scan line it was shown that on the selected ROI there was more variation of the gray scales on the processed mammogram which verifies that the contrast was improved in the local region of the mammogram.

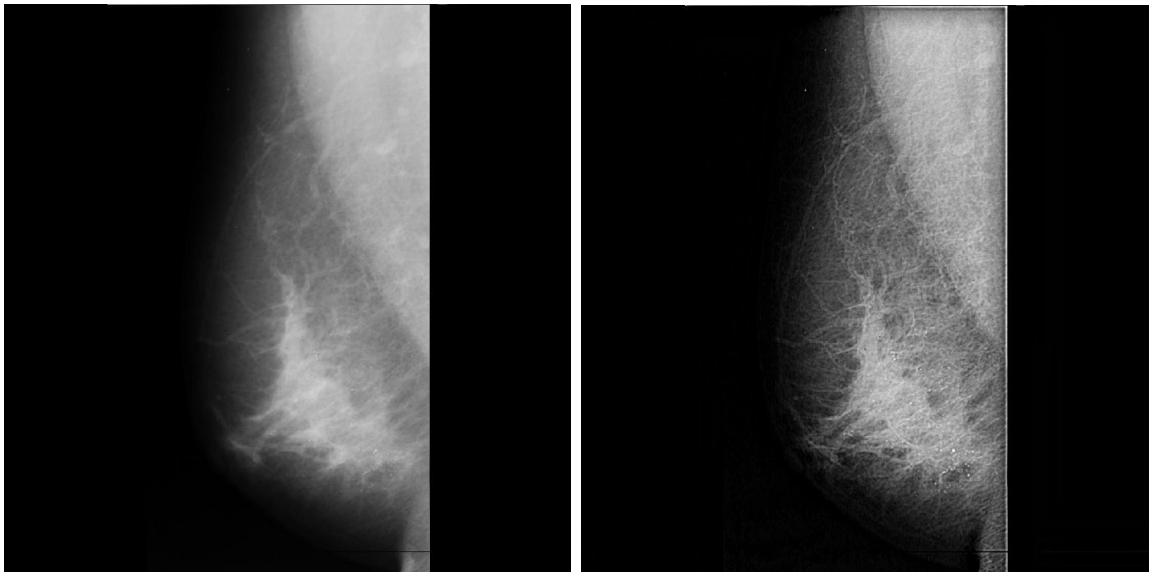

Figure 4.5. (a) shows the original mammogram with fatty-glandular tissue that containing malignant calcification, and Figure 4.5. (b) shows the processed image.

The histogram of the original image and the processed image is shown in Figure 4.6 (a) and Figure 4.6 (b).

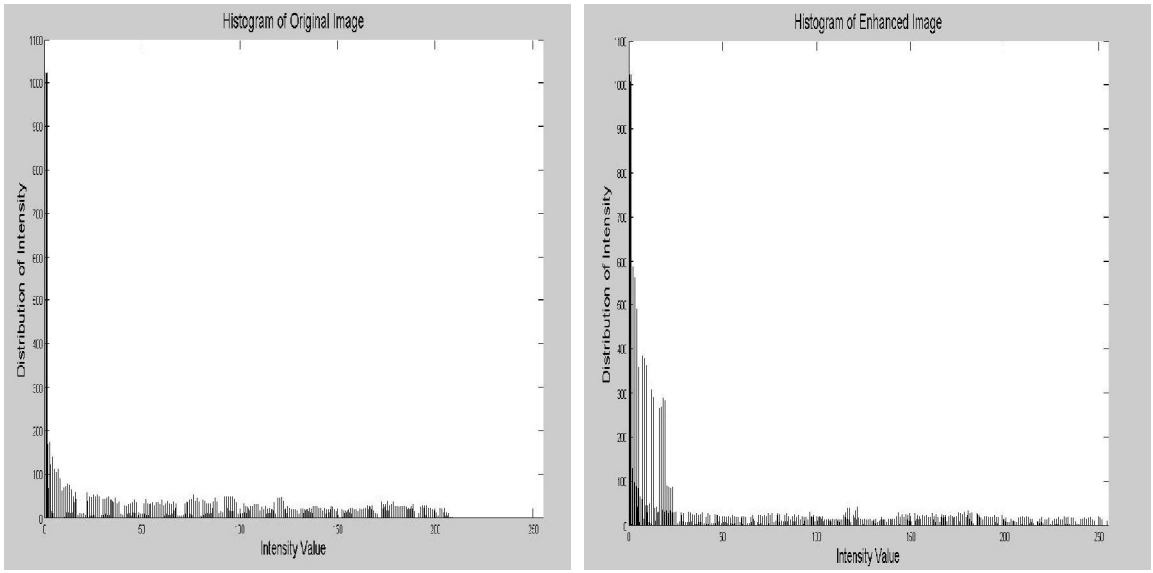

Figure 4.6. (a) shows the histogram of the original image, and Figure 4.6. (b) shows the histogram of the processed image.

The ROI of the original image and the ROI of the processed image is shown in Figure 4.7 (a) and Figure 4.7 (b). The scan lines are shown in Figure 4.8 (a) and Figure 4.8 (b).

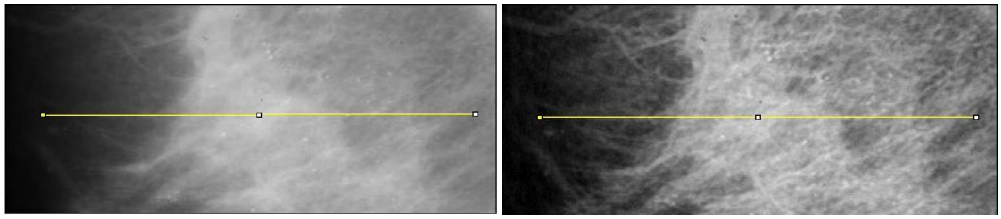

Figure 4.7. (a): ROI of original image, and Figure 4.7. (b) ROI of processed image for plotting line profile

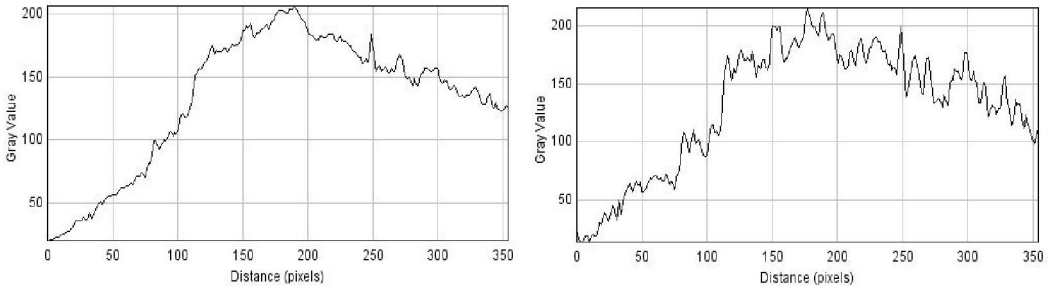

Figure 4.8. (a): shows the line profile of original mammogram, and Figure 4.8. (b) shows the line profile of the processed mammogram

4.2. QUANTITATIVE PERFORMANCE EVALUATION

For verifying the contrast enhancement, some quantitative measurement is performed. The SNR, CNR, DSM, TBC_s, TBC_e and D for both cases are shown in table 4.1.

From the table, it is clearly seen that in case 1, the enhanced image has better contrast compare to original image. The SNR value is 18.42 dB. The higher SNR value represents that the object is more visible when the contrast is large enough to overcome the random noise.

Table 4.1. Quantitative values of the enhanced image

Case	SNR	CNR	DSM	TBC_s	TBC_e	D
Case 1	18.42	54.0593	19.96	0.4635	0.917	18.97
Case 2	16.96	91.07	11.70	1.47	0.962	10.71

Therefore higher SNR value of the enhanced image represents better contrast than the original image. The CNR value for the first case is 54.0593 which mean the image features are more visible from its surroundings. The DSM of the enhanced image is found as 19.96. Since higher DSM represents a better enhancement so it can be claimed that the contrast has improved. Also from Figure 4.9 it is clear that the overlap between the PDFs are less which means separation of background and object is more. This also proves the enhancement of the image.

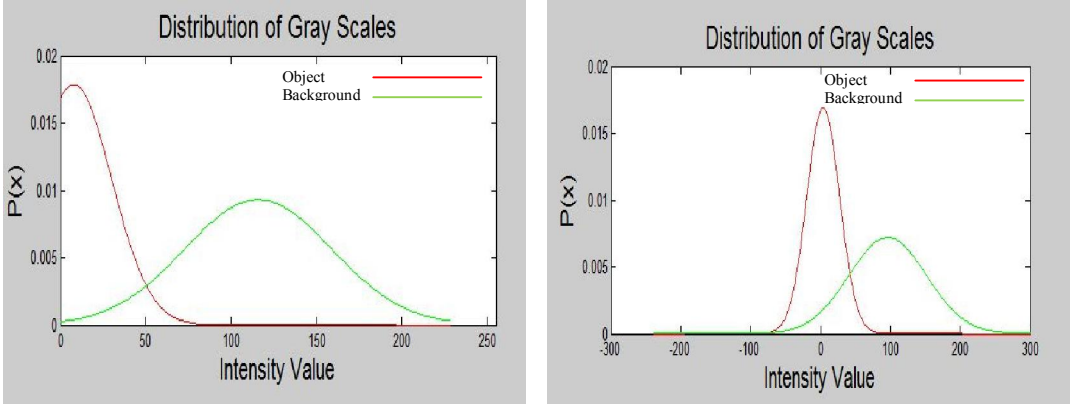

Figure 4.9 (a) shows the PDF of original image, and Figure 4.9 (b) shows the PDF of enhanced image (Case 1)

The TBCs value of the enhanced image is 0.4635 and the TBCe value of the enhanced image is 0.917. Both values are greater than zero prove that the output image is enhanced properly. Also, the combined enhancement measure, D is 18.97. Since the DSM

is much higher, the D value will also be higher. The value of D is mainly used for comparing image processing techniques.

In case-2, the SNR value is 15.34 dB which proves the enhancement of the mammogram. The DSM of the enhanced image is found as 11.70. Since higher DSM represents better enhancement so we can say that the contrast is improved. The CNR value is 91.07 which represents better enhancement. Also from Figure 4.10, it is clear that the overlap between the PDFs are less which means separation of background and object is more. This also proves the enhancement of the image.

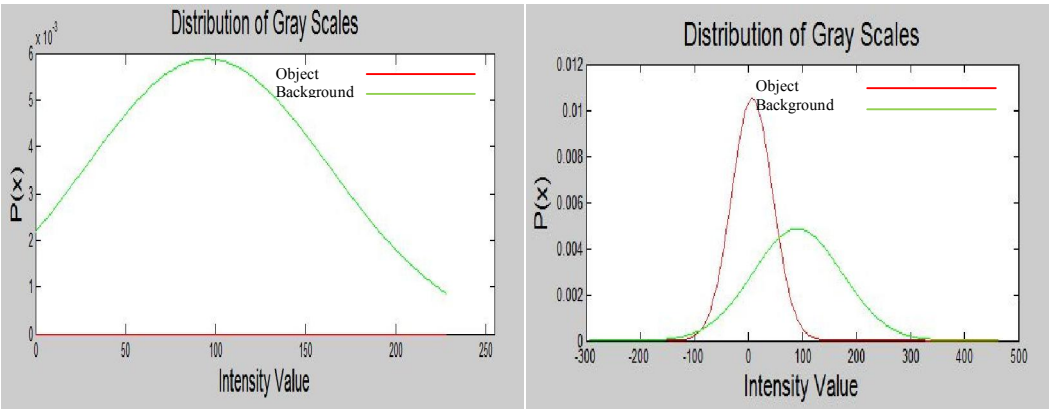

Figure 4.10 (a) shows the PDF of original image and Figure 4.10. (b) shows the PDF of enhanced image (Case 2)

The TBCs value of the enhanced image is greater than 1 which also proves the enhancement criteria. The TBCe value of the enhanced image is 0.962 that also greater than zero proves the validity of the new contrast enhancement technique.

5. DISCUSSION

The proposed image processing algorithm attempts to improve contrast of digital mammogram by enhancing image feature based on multi-scale decomposition. Several well-known image processing techniques, histogram equalization (HE), contrast limited adaptive histogram equalization (CLAHE), and multi-scale image contrast amplification (MUSICA^{TM}), were compared with the proposed algorithm.

In case 1, the result of HE is shown in Figure 5.1 (a). It enhances the contrast, but the image quality decreases. The detailed information of the image was lost and noise in the image increased. From Table 5.1, it was seen that the SNR was negative. The contrast was improved but the overall appearance of the image was severe. Also, the DSM value was positive but the value was less than the value of the new technique. Also, the TBCs value should be greater than zero, but here the value was negative.

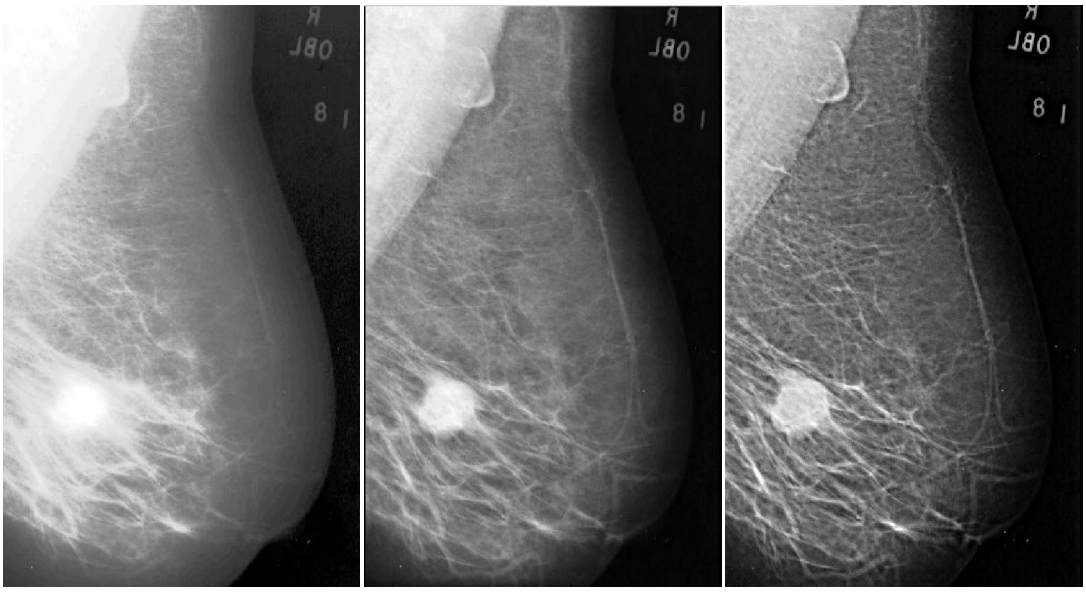

Figure 5.1. (a) shows the result of HE, Figure 5.1. (b) shows the result of CLAHE, and Figure 5.1. (c) shows the result of MUSICA (case-1)

The enhancement result of CLAHE is shown in Figure 5.1 (b). The enhancement is better than HE, and SNR is 15.34 dB which means the noise is suppressed from the original feature of the image. The proposed algorithm had an SNR value 16.78 dB which indicates the result was better than CLAHE. Although, the CNR value was less in the new algorithm, the DSM value was greater than CLAHE. The combined enhancement measure was also higher than both HE and CLAHE which established the validity of the proposed algorithm. The result of MUSICA was shown in Figure 5.1 (c). The SNR value is higher in the proposed algorithm and the quantitative data also proved that the proposed technique has superiority over conventional algorithms.

In the second case, similar comparison was performed as shown in Figure 5.2 and the final outcome was that the new image processing algorithm is promising for contrast enhancement of digital mammography than the traditional approaches. The calcification in the mammogram is visible to the human eye, which was not seen in the original image. A clinical study is needed to verify the proposed technique. Image contrast enhancement is a subjective process. Although, some metrics can verify the result but the contrast enhancement should be qualified by human visual system.

Table- 5.1: Quantitative comparison of new technique with traditional techniques.

Case	Methods	SNR (dB)	CNR	DSM	TBC_s	TBC_e	D
Case 1	HE	-0.977	175.93	24.08	-1.81	Inf	23.03
	CLAHE	15.34	120.94	2.88	11.60	Inf	10.77
	MUSICA	15.50	54.15	15.98	0.60	-10.17	11.05
Case 2	HE	-4.67	198.77	18.50	4.008	Inf	17.76
	CLAHE	20.89	100.82	3.35	8.21	Inf	3.23
	MUSICA	14.733	86.37	17.53	5.58	-15.26	7.90

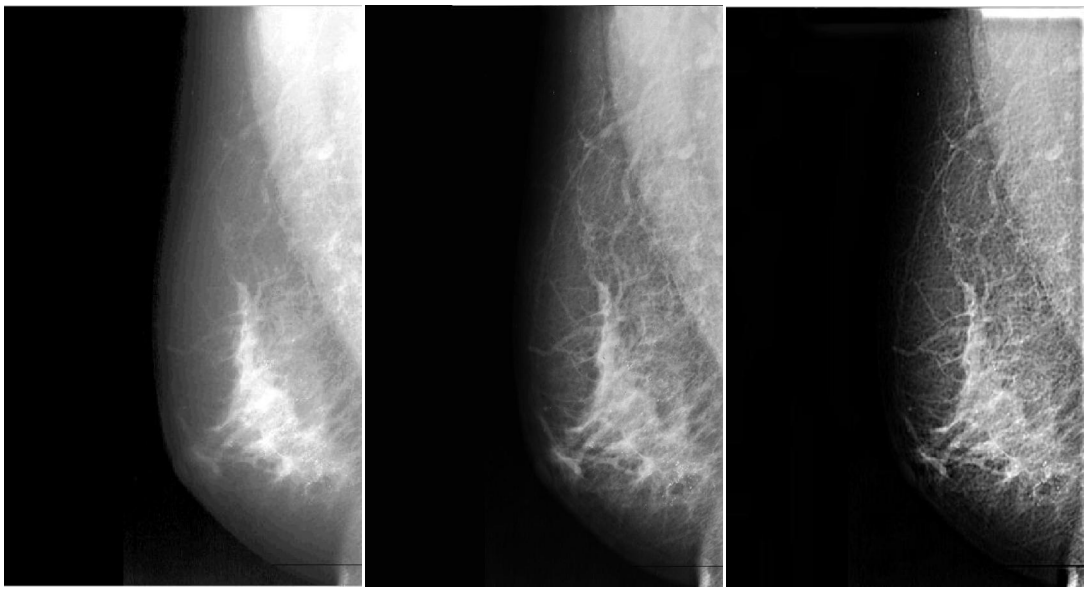

Figure 5.2 (a) shows the result of HE, Figure 5.2 (b) shows the result of CLAHE, and Figure 5.2 (c) shows the result of MUSICA (case-2)

6. CONCLUSION

A contrast enhancement technique for digital mammography based on a multi - scale Laplacian pyramid is proposed. Several mapping functions based on empirical analysis were developed to enhance the subtle contrast of the digital mammogram. Since, subtle information such as, calcifications lie on different scales, this technique has special importance in digital mammography. The method enhances both the global and local features of the image by suppressing noise content of the image. Conventional image processing algorithms were compared experimentally with the proposed image processing algorithm which proves the acceptance of the algorithm for enhancing the contrast of digital mammography. The proposed method would be helpful for other image processing applications.

APPENDIX
MATLAB CODE

```
clc                                    % clear Command Window
clear all                              % Clear all Variables
close all                              % Close all Figures
I0= imread('mdb028.pgm');              % Read Image from Directory
K0= 50;                                % Upper Bound of Level 1
K1=97;                                 % Upper Bound of Level 2
K2= 40;                                % Upper bound of Level 3
K3= 0;                                 % Upper Bound of Level 4
K4= 2;                                 % Upper Bound of Level 5
Ip= padarray(I0,[16 16],'replicate','both');% Pad the image
Ip= double(Ip);                                % Convert to Double Precision
sigma=.7;                              % Selection of sigma in Gaussian Kernel
for i= -7:7
for j= -7:7
A (i+8, j+8)= (1/(2*pi*sigma^2)).*exp (-(i^2+j^2)./(2*sigma^2));
                                       % Generation of Gaussian Kernel
end
end
gauss= A./sum(A(:));                   % sum of all Gaussian components equals 1
blur= conv2(Ip, gauss,'same'); % convolution of the image
DSI128= imresize(blur,.5,'bicubic'); % Downsampling the image
im1_256= imresize(DSI128,2,'bicubic'); % Upsampling the image
im2_256= conv2(im1_256, gauss, 'same'); % Convolution
L0 = Ip- im2_256;                      % Laplacian Image at Level 1 generated
gamma1=.1;                             % Selection of non-linear exponents
ind= find(L0<K0); % Finding coefficients that are less than upper bound
L0(ind)= 1.5*L0(ind)+sign(L0(ind)).*(abs((L0(ind).*
(max(L0(:)))).^gamma1)).*(max(L0(:))/K0);
```

```
                                        % enhance the Laplacian Coefficients
ind1= find(L0>K0); % Coefficients that are greater than upper bound
L0(ind1)= .8*L0(ind1); % Attenuating Laplacian Coefficients
blur128= conv2(DSI128, gauss, 'same'); % Gaussian Image of level 2
DSI64= imresize(blur128,.5, 'bicubic');  % Downsampling Image
im1_128= imresize(DSI64,2, 'bicubic'); % Upsampling the image
im2_128= conv2(im1_128,gauss,'same'); % Convolution
L1= DSI128-im2_128;                     % Laplacian Image of Level 2
L1= 5*L1;                               % Modified Laplacian Coefficients
blur64= conv2(DSI64, gauss, 'same');    % Convolution
DSI32= imresize(blur64,.5, 'bicubic');   % Downsampling
im1_64= imresize(DSI32,2, 'bicubic');  % Upsampling
im2_64= conv2(im1_64,gauss,'same');   % Convolution
L2= DSI64-im2_64;                       % Laplacian Image of Level 3
gamma5=.1;                              % non-linear exponent
L2= .05*L2+ sign(L2).*(abs((L2.*(max(L2(:)))).^gamma5));
                                        % Modified Laplacian Coefficients at Level 3
blur32= conv2(DSI32, gauss, 'same');   % Convolution
DSI16= imresize(blur32,.5, 'bicubic');    % Downsampling
im1_32= imresize(DSI16,2, 'bicubic');    % upsampling
im2_32= conv2(im1_32,gauss,'same');    % Convolution
L3= DSI32-im2_32;                       % Laplacian Image at Level 4
gamma8=.9;                              % Non-linear exponent
ind= find(L3<K3);                   % Finding Coefficients less than upper bound
L3(ind)= 4*L3(ind);                     % Modification of coefficients
ind1= find(L3>K3);                      % finding Coefficients greater
                                                than upper bound
L3(ind1)=.01*sign(L3(ind1)).*(max(L3(:))-(K3-
(abs(L3(ind1)).^gamma8))).*(max(L3(:)/2)./(max(L3(:))-K3)); % Modification
blur16= conv2(DSI16, gauss, 'same');                % Convolution
DSI8= imresize(blur16,.5, 'bicubic');               % Downsampling
```

```
im1_16= imresize(DSI8,2, 'bicubic');                    % Upsampling
im2_16= conv2(im1_16,gauss,'same');                     % Convolution
L4= DSI16-im2_16;                                       % Laplacian Image at Level 5
gamma10=.3;                                             % Non-linear exponent
ind= find(L4<K4);      % finding coefficients less than upper bound
L4(ind)= 1.8*L4(ind);                                   % Modified Laplacian Coefficients
ind1= find(L4>K4);                                      % Finding Coefficients greater than Upper bound
L4(ind1)=.05*sign(L4(ind1)).*(max(L4(:))-(K4-(abs(L4(ind1)).^gamma10))).*
(max(L4(:)/2)./(max(L4(:))-K4)); % Modified laplacian Coefficients
R4= im2_16+L4;                                          % Reconstruction
USI16= imresize(R4, 2, 'bicubic');                      % Upsampling
Rblur16= conv2(USI16,gauss,'same');                     % Convolution
R3= Rblur16+L3;                                         % Reconstruction
USI32= imresize(R3, 2, 'bicubic');                      % Upsampling
Rblur32= conv2(USI32,gauss,'same');                     % convolution
R2= Rblur32+L2;                                         % Reconstruction
USI64= imresize(R2, 2, 'bicubic');                      % Upsampling
Rblur64= conv2(USI64,gauss,'same');                     % Convolution
R1= Rblur64+L1;                                         % Reconstruction
USI128= imresize(R1, 2, 'bicubic');                     % Upsampling
Rblur128= conv2(USI128,gauss,'same');                   % Convolution
R0= Rblur128+L0;                                        % Reconstruction
R0(1:16,:)=[];                                          % Removing Pad
R0(:,1:16)=[];                                          % Removing Pad
R0(1025:end,:)=[];                                      % Removing Pad
R0(:,1025:end)=[];                                      % Removing Pad
figure, imshow(uint8(R0),[]);                           % Final Image
```

BIBLIOGRAPHY

[1] Bick U., F. Diekmann, "*Digital Mammography Book*," Springer-Verlag Berlin Heidelberg, 2010.

[2] Breast Cancer organization, *"<http://www.breastcancer.org /symptoms /understand_bc/statistics.jsp>,"* Accessed September 17, 2011.

[3] Burt Peter J., Edward D. Adelson, "The Laplacian Pyramid as a Compact Image Code," *IEEE Transactions on Communications,* 1983. Vol. 31, No. 4, 532-540.

[4] Chen S. D., and A. R. Ramli, "Contrast enhancement using recursive meanseparate histogram equalization for scalable brightness preservation," *IEEE Trans. Consumer Electronics*, November 2003, Vol. 49, No. 4, 1301-1309.

[5] Chen Soong-Der, and A. R. Ramli, "Minimum mean brightness error bihistogram equalization in contrast enhancement," *IEEE Transactions on Consumer Electronics,* 2003, Vol. 49, No. 4, 1310-1319.

[6] Cheng H. D., Huijuan Xu, "A novel fuzzy logic approach to mammogram contrast enhancement," *Information Sciences,* 2002, Vol. 148, 167-184.

[7] Delaney Alexander H. and Y. Bresler, "Multiresolution Tomographic Reconstruction using Wavelets," *IEEE Transactions on Image Processing*, 1995, No. 6, 799–813.

[8] Dhawan A., Gianluca Buelloni and Richard Gordon, "Enahncement of Mammographic Feature by Optimal Adaptive Neighborhood Image Processing," *IEEE Transaction on Medical Imaging,* 1986, Vol. 5 No. 1, 8-15.

[9] Dippel Sabine, Martin Stahl, Rafael Wiemker, Thomas Blaffert, "Multiscale Contrast Enhancement for Radiographies: Laplacian Pyramid versus Fast Wavelet Transform*", IEEE Transaction on Medical Imaging,* Vol. 21, No. 4, 2002, 343-353.

[10] Dyer Charles, "Multiscale Image Understanding Computer Science," *Technical Report# 679*, Computer Science Department, University of Wisconsion, Madison, 1986.

[11] Gonzalez R.C. and Richard E. Woods, "*Digital Image Processing*," Addison-Wesley Longman Publishing Co., Inc., Boston, MA, USA, 2008.

[12] Haus AG, Yaffe MJ., "Screen-film and Digital mammography: Image Quality and Radiation Dose Considerations," *Radiol Clin North America, 2000*, 38:871– 898.

[13] Heinlein Peter, Johann Drexl, and Wilfried Schneider, "Integrated Wavelets for Enhancement of Microcalcifications in Digital Mammography," *IEEE Transactions On Medical Imaging,* 2003, Vol. 22, No. 3, 402-413.

[14] Hendrick RE, Berns EA., "Optimizing techniques in screen-film mammography," *Radiol Clin North America,* 2000, 38:701–718.

[15] Kim Y.K. , L. S. Kim, and S. H. Hwang, "An advanced contrast enhancement using partially overlapped sub-block histogram equalization," *IEEE Transactions on Circuits and Systems for Video Technology*, 2001, Vol. 11, No. 4, 475-484.

[16] Laine A., Jian Fan and Wuhai Yong, "Adaptive Multiscale Processing for Contrast Enhancement," *SPIE*, 1993, Vol 1905/521, 521-532.

[17] Loza A., david Bull, Alin Achim, "Automatic Contrast Enhancement of Low-Light Images Based on Local Statistics of Wavelet Coefficients," *IEEE 17th International Conference on Image Processing*, 2010, 3553-3556.

[18] Mahesh Mahadevappa, "Digital Mammography: An Overview," *RadioGraphics, RSNA 2004*, Vol 24, No. 6, 1747-1760.

[19] Mainardi L., K. Passera, A. Lucesoli, D. Vergnaghi, G. Trecate, E. Setti, R. Musumeci, and S. Cerutti, "A nonrigid registration of breast MR images using complex-valued wavelet transform," *Journal of Digital Imaging*, 2007, PMCID: PMC3043828, 27-36.

[20] Pajak Dawid, Martin Cadik, et al, "Contrast Prescription for Multiscale Image Editing," *The Visual Computer*, 2010, Vol. 26, No. 6-8, 739-748.

[21] Paquin D., "Multiscale Method for Image Registration," *Doctor of Philosophy Dissertation of the Department of Mathematics at Stanford University*, 2007.

[22] Pisano ED, Yaffe MJ, Hemminger BM, et al., "Current status of full-field digital mammography*," Academic Radiology,* 2000, Vol. 7, 266–280.

[23] Pisano et al, "*Digital Mammography*," Lippincott Williams and Wilkins*,* Philadelphia, PA, USA, 2004.

[24] Pisano Etta D., Shuquan Zong, Bradley M. Hemminger, Marla DeLuca, Eugene Johnston, Keith Muller, M. Patricia Braeuning, Stephen M. Pizer, "Contrast Limited Adaptive Histogram Equalization Image Processing to Improve the Detection of Simulated Spiculations in Dense Mammograms," *Journal of Digital Imaging*, Vol. 11, No. 4, 193-200.

[25] Porter R. and N. Canagarajah, "A robust automatic clustering scheme for image segmentation using wavelets," *IEEE Transactions on Image Processing,* 1996, No. 4, 662–665.

[26] Rowlands JA, Hunter DM, Araj, N., "X-ray imaging using amorphous selenium: a photoinduced discharge readout method for digital mammography," *Medical Physics,* 1991, 18:421–431.

[27] Singh Sameer, Member, IEEE, and Keir Bovis, "An Evaluation of Contrast Enhancement Techniques for Mammographic Breast Masses," *IEEE Transactions on Information Technology in Biomedicine,* 2005, Vol. 9, No. 1, 109-119.

[28] Stahl Martin, Til Aach, Sabine Dippel, thorsten Buzug, Raphael Wiemker, Ulrich Neitzel, "Noise Resistant Weak-Structure Enhancement for Digital Radiography," *Proceedings of SPIE,* Vol. 3661, 1406-1417.

[29] Vuylsteke Pieter, Emile Schoeters, "Multiscale Image Contrast Amplification (MUSICA^{TM})," *SPIE,* Vol 2167, 551-560.

[30] White J., "FDA approves system for digital mammography," *National Cancer Institute,* 2000; Vol. 92, Issue 6, 442.

[31] Wu Zhe, Julong Yuan, Binghai Lv, Xiaofeng Zheng, "Digital Mammography Image Enhancement using Improved Unsharp Masking Approach," *3rd International Congress on Image and Signal Processing*, 2010, 668-672.

[32] Yeong-Taeg K., "Contrast enhancement using brightness preserving bi-histogram equalization*," IEEE Transactions on Consumer Electronics*, 1997, Vol. 43, No. 1, 1-8.

VITA

Muhammad Imran Khan Abir was born on October, 1987, in Tangail, Bangladesh. He received his Bachelor of Science in Mechanical Engineering from Bangladesh University of Engineering and Technology, Dhaka, Bangladesh in October 2009. After graduation, he joined in an oil refining company, Eastern Refinery Ltd., at Chittagong, Bangladesh and worked there for 4 months. Being a part of researcher, he joined to Missouri University of Science and Technology (Missouri S&T) for pursuing his M.S. in Nuclear Engineering. He is planning to pursue his PhD after finishing his M.S.

Abir held a Graduate Research Assistantship under Dr. Hyoung Koo Lee with the department of Nuclear Engineering at Missouri S&T. He received his Master of Science in Nuclear Engineering from Missouri University of Science and Technology in December 2011.